1986

Apodization of Surface Acoustic Wave Three Phase Unidirectional Transducers

Benjamin P. Abbott
University of Central Florida

APODIZATION OF SURFACE ACOUSTIC WAVE THREE PHASE UNIDIRECTIONAL TRANSDUCERS

BY

BENJAMIN PAUL ABBOTT
B.S.E., University of Central Florida, 1984

THESIS

Submitted in partial fulfillment of the requirements
for the degree of Master of Science in Engineering
in the Graduate Studies Program of the College of Engineering
University of Central Florida
Orlando, Florida

Spring Term
1986

ABSTRACT

This thesis presents an introduction to surface acoustic wave (SAW) unidirectional transducer (UDT) apodization. An unbalanced apodization structure is described. The structure is shown to suffer from unbalanced capacitive effects, significant apodization losses and passband ripple. A balanced UDT structure is developed for the purpose of improving performance and minimizing undesirable effects associated with the unbalanced structure.

Each apodization structure is analyzed and compared using a typical impulse response of a SAW transducer. The analysis is accomplished using SAWCAD2, a unidirectional Surface Acoustic Wave Computer Aided Design FORTRAN-77 program developed at the University of Central Florida. Having shown the balanced structure to be superior in performance, this structure is described in greater detail and a short summary of UDT fabrication is given.

ACKNOWLEDGEMENTS

I would like to acknowledge Don Malocha and Sam Richie for the many hours they spent writing the original FORTRAN code for SAWCAD2 and STRUCTURE. I would also like to acknowledge Dr. Malocha's assistance and guidance in the preparation of the thesis. Finally, I acknowledge the support of my family, friends and the members of the research group in the Solid State Devices and Systems Lab at the University of Central Florida, to which I belong.

TABLE OF CONTENTS

LIST OF FIGURES

CHAPTER I

INTRODUCTION

The three phase unidirectional transducer (UDT) was developed in the early 1970s by Clinton S. Hartman and his associates, W. Stanley Jones and Howard Vollers [1].

The development of UDT technology overcame a major drawback of bidirectional transducers (BDTs). BDTs launch energy in two directions, both toward and away from the receiving transducer. As a result, a BDT is only 50% efficient. The UDT, however, only launches energy in one direction, toward the receiving transducer. The ability to launch energy in one direction eliminated 3 dB of acoustic power loss in each transducer, or 6 dB of acoustic power loss for a typical Surface Acoustic Wave (SAW) filter.

In addition to the development of the three phase UDT, several other UDT technologies were developed. These include the group type UDT [2], the quadrature four phase UDT [3], the quadrature three phase UDT [4] and the natural single phase UDT [5]. The three UDT offers several advantages over all of these UDT technologies. The three phase UDT lacks the resistive losses and spurious passband responses of the group type UDT. The three phase requires only four components for phasing and matching, and offers a higher first harmonic implementation than the quadrature three and four phase

UDTs. The natural single phase UDT at present is not truely unidirectional (15 dB unidirectionality at synchronous frequency) and does not offer wideband unidirectional behavior [5].

Unlike other SAW technologies such as BDTs, natural single phase UDTs and group type UDTs, the three phase UDT requires that metalized bridges be used to interconnect electrodes of the same voltage phase. Therefore, accompanying the advantages of low insertion loss are more complex fabrication techniques. In addition, narrow transition bandwidths have been more difficult to implement in UDTs than in BDTs due to the required development of a satisfactory apodization technique for the UDT.

Presently, two weighting techniques are used in UDT technologies: withdrawal weighting [6] and the apodization of transducers with all taps aligned to one side of the transducer [7]. However, both of these weighting techniques have drawbacks. Withdrawal weighting results in a very nonoptimum time-bandwidth product and the conventional UDT apodization technique results in unbalanced capacitive effects, significant apodization losses [8] and passband ripple.

The purpose of this thesis is to describe a method by which apodization may be implemented in a UDT without introducing significant apodization losses, passband ripple and maintaining a capacitively balanced structure. In addition, this apodization structure shall be compared with the conventional unbalanced apodization structure through the use of an example.

In order to present this comparison, a detailed analysis of each apodization structure is needed. SAWCAD2 [9], a three phase UDT computer-aided design and analysis program, will be used for this analysis. Several updates to SAWCAD2 were required to perform the desired analysis of these structures. These updates include, first, a revision to the array factor; second, a revision to the element factor; and third, the inclusion of the analysis of apodization effects. These updates are discussed in greater detail in Chapter II.

CHAPTER II

REVISIONS TO SAWCAD2

Review of SAWCAD2

In order to investigate the effects of various apodization techniques on the performance of UDTs, modifications were made to SAWCAD2.

SAWCAD2 is a UDT surface acoustic wave computer-aided design and analysis software package written in FORTRAN-77. SAWCAD2 is capable of generating the necessary time impulse responses for the implementation of finite impulse response bandpass filters, such as SAWs. SAWCAD2, as originally written, performed the analysis of amplitude weighted devices given an impulse response sampled at three times the synchronous frequency of the device. However, this analysis required that negative tap weights be implemented in the device's structure. The array factor tap weights are restricted to be non-negative. The original SAWCAD2 had an oversight in the conceptual understanding of the requirements of the array factor. This oversight occurred as a result of a lack of an accurate definition of the array factor in the existing literature on SAWs. In addition, the element factor used was simply a close approximation.

The changes to SAWCAD2 include corrections to the array factor and element factor and the implementation of the analysis of

apodization effects. The exact nature of the apodization effects, the element factor and the array factor shall be presented in detail in the following sections of this chapter.

Array Factor

The desired ideal impulse response is defined by:

$$h(t) = \sum_{n=1}^{N} b_n \cdot \delta(t - t_n) \qquad (2\text{-}1)$$

The array factor, a(t), is extracted from h(t) by zeroing all negative b_n values. The array factor is defined quantitatively by equation (2-2).

$$a(t) = \sum_{n=1}^{N} a_n \cdot \delta(t - t_n) \qquad (2\text{-}2)$$

where:

$a_n = b_n$, if $b_n > 0$

$a_n = 0$, otherwise

The nature of the array factor results from the operation of a physical electrode. A single electrode, such as the one in Figure 2.1, may only generate a positive response. The physical electrode does not contain any phase information. All phase information must be contained spatially and/or in time. Electrodes are spatially

phased by placing them at specific locations within the transducer. This is illustrated in Figure 2.2.

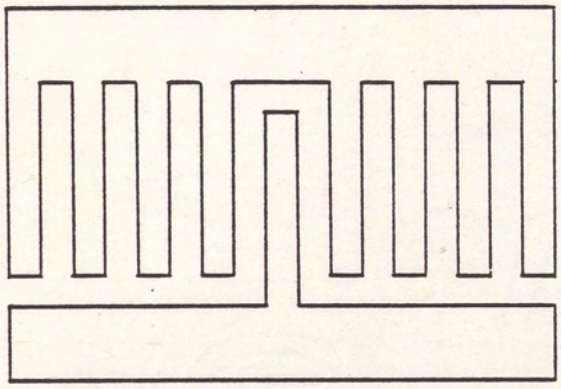

Figure 2.1. A Single Positive Electrode.

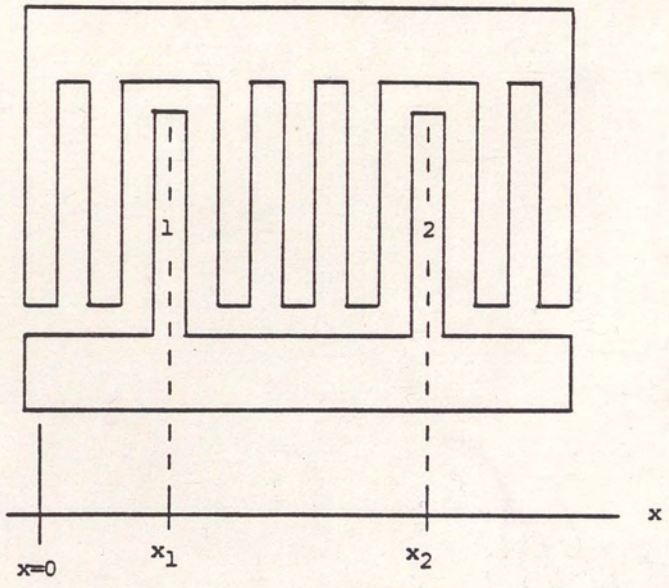

Figure 2.2. Spatial Phasing of Electrodes.

Given an acoustic velocity, v_a, the spatial phase, θ_1, of the first electrode in Figure 2.2 is defined by:

$$\theta_1 = e^{+jkx_1} \tag{2-3}$$

The spatial phase, θ_2, of the second electrode is given by:

$$\theta_2 = e^{+jkx_2} \tag{2-4}$$

where:

$k = 2 \cdot \pi/\lambda$ = wave number

$\lambda = v_a/f$

f = frequency of the acoustic wave

The response of an electrode may be phased in time by phasing the voltage applied to the electrode. This is illustrated in Figure 2.3.

If V_1 is chosen as the reference phase, then the phase of the second electrode lags the first by $\theta(w)$.

In the analysis of a SAW device, spatial phasing is implemented by associating an appropriate time delay t_n with its respective tap weight a_n, as defined by equation (4-4). Voltage phasing must be implemented using a multiphase transducer. In multiphase transducers, one phase must always be used as a potential reference, generally the ground phase, and another phase as the voltage phase reference.

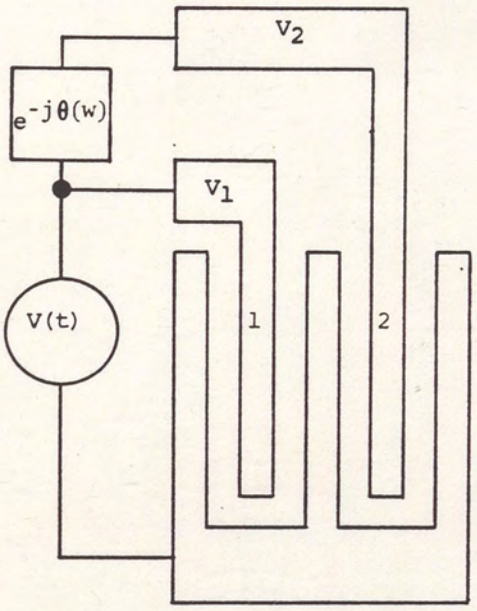

Figure 2.3. Voltage Phasing of Electrodes.

Therefore, voltage phasing requires that the transducer have at least three voltage phases. In a three phase UDT, there are three voltage phases present. SAWCAD2 uses one of these phases as the potential reference, ground, another as the voltage phase reference, V_1. The remaining voltage phase, V_2, is phased with respect to V_1 in order to obtain the unidirectional behavior of the device.

Element Factor

The ideal response of a transducer is the transducer's array factor. Due to interactions between adjacent electrodes and finite electrode widths, this response is distorted. The acoustic response,

u(t), of an array of electrodes may be found by convolving the array factor, a(t), with the actual impulse response, e(t), of a single electrode. This is given by:

$$u(t) = a(t) * e(t) \tag{2-5}$$

The acoustic impulse response, e(t), of a single electrode such as the one in Figure 2.4(a) is shown in Figure 2.4(b). The impulse response, e(t), is derived from the charge distribution present on the array of electrodes, for the signal incident on the array being an impulse [10].

Since convolution in time is equivalent to multiplication in frequency, equation (2-5) may be written in the frequency domain as:

$$U(f) = A(f) \cdot E(f) \tag{2-6}$$

The function E(f) is known as the element factor. The normalized element factor derived from [10] may be written as:

$$E(f) = \frac{\sin(\pi s_o)}{P_{-s_o}[-\cos(\eta\pi)]} \cdot P_n[\cos(\eta\pi)] \cdot P_{-\frac{1}{2}}[-\cos(\eta\pi)] \tag{2-7}$$

where:

$P_v(x)$ = the Legendre polynomial of x and order v

n = integer portion of f/f_s

s_o = fractional portion of f/f_s

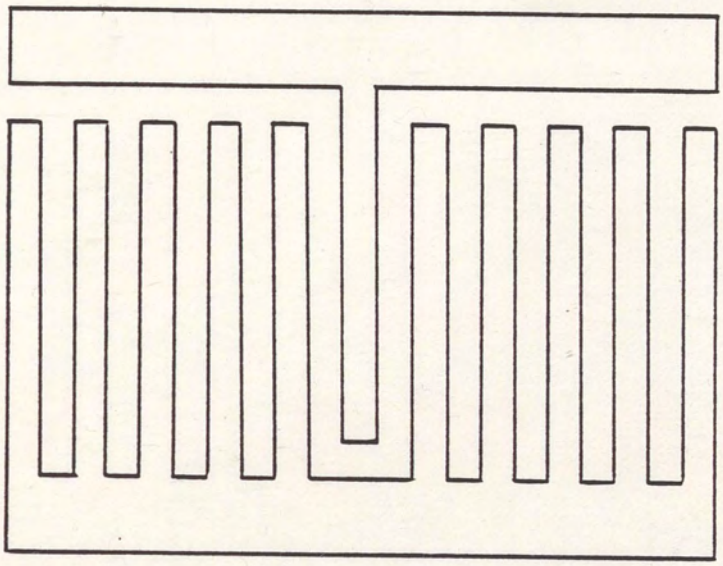

Figure 2.4(a). Array of Electrodes.

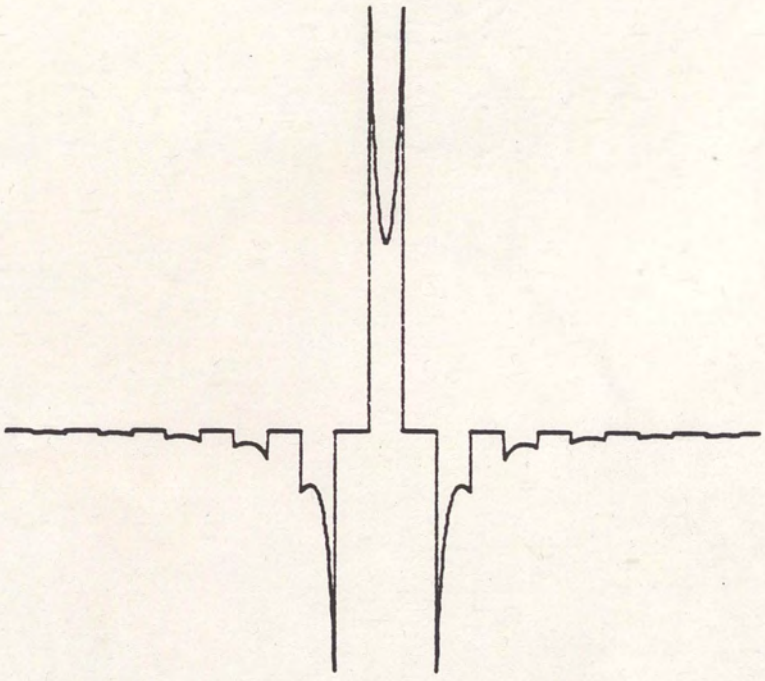

Figure 2.4(b). Charge Distribution. Charge Distribution of the Effective Impulse Response of the Array of Electrodes in (a).

η = metalization ratio, a/p

a = width of an electrode

p = period of the electrodes

f_s = sampling frequency

The quantities "a" and "p" are illustrated graphically in Figure 2.5. The element factor, for a 50% metalization ratio, normalized at its synchronous frequency, is plotted in Figure 2.6. The frequency axis of Figure 2.6 has been normalized to the sampling frequency, f_s.

Apodization Effects

Apodization is a method of weighting a SAW transducer through the modulation of the lengths of the transducer's electrodes. An example impulse response is given by h(t) as:

$$h(t) = 0.25 \cdot \delta(t + 3t_o) + 0.50 \cdot \delta(t + 2t_o) + 0.75 \cdot \delta(t + t_o)$$
$$+ 1.00 \cdot \delta(t) + 0.75 \cdot \delta(t - t_o) + 0.50 \cdot \delta(t - 2t_o)$$
$$+ 0.25 \cdot \delta(t - 3t_o) \qquad (2\text{-}8)$$

An apodization pattern implementing the impulse response in equation (2-8) is shown in Figure 2.7.

The transducer is arbitrarily divided into four channels, as shown in Figure 2.7. The response received by the unapodized transducer is the sum of the responses radiated by each channel. Therefore, the impulse response h(t) may be written as the

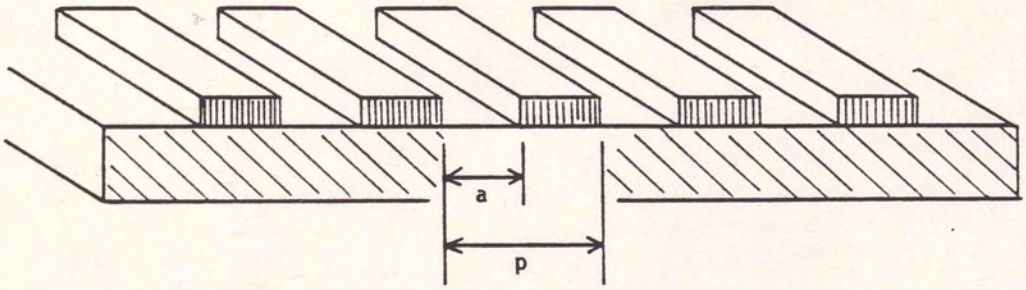

Figure 2.5. Cross-section of a SAW Transducer.

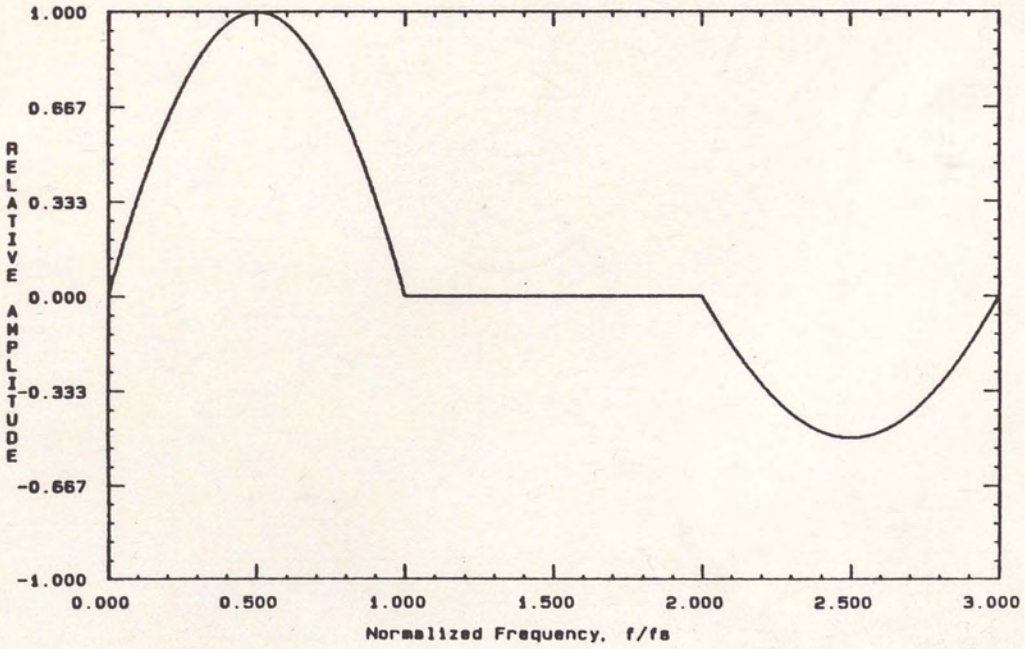

Figure 2.6. Element Factor Normalized at $f_s/2$ and Plotted for f = 0 to $3f_s$ and a Metalization Ratio of 50%.

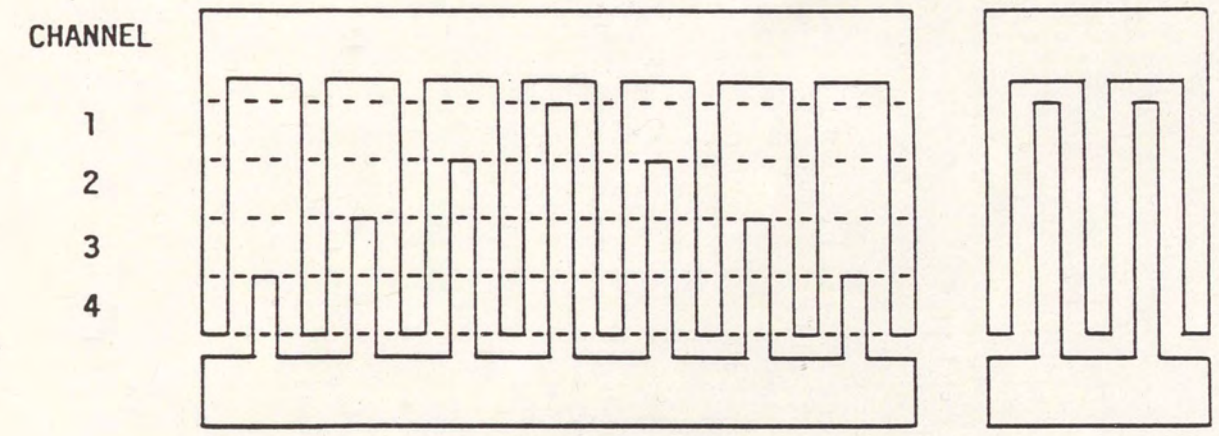

Figure 2.7. Sample Apodized Transducer.

superposition of all the channels. The ideal impulse response of the apodized transducer, using the superposition of the four channels, is given by:

$$h(t) = \sum_{i=1}^{4} \tfrac{1}{4} \cdot h_i(t) \qquad (2\text{-}9)$$

where $h_i(t)$ is the impulse response of the ith channel whose tap weights are restricted to the values of 0 and 1.

From Parseval's theorem, the transmitted and received energies may be written, respectively, as:

$$E_t = \sum_{i=1}^{M} \frac{1}{M} \cdot |H_i(f)|^2 \qquad (2\text{-}10)$$

$$E_r = \left| \sum_{i=1}^{M} \frac{1}{M} \cdot H_i(f) \right|^2 \qquad (2\text{-}11)$$

Equations (2-10) and (2-11) are normalized for a 1 ohm load.

Unless $H_i(f) = H_{i+1}(f)$ for all i, more energy will be transmitted than received. As a result, the efficiency of the device will be impacted. As a result, at the synchronous frequency of the device, there is an inherent insertion loss in the device. This insertion loss has been termed apodization loss [8] and is normally specified in dB. Apodization loss is calculated from [8]:

$$\text{Apodization Loss} = -10 \cdot \text{Log}_{10} \left\{ \frac{\left| \sum_{i=1}^{M} \frac{1}{M} \cdot H_i(f_o) \right|^2}{\sum_{i=1}^{M} \left| \frac{1}{M} \cdot H_i(f_o) \right|^2} \right\} \qquad (2\text{-}12)$$

For the transducer illustrated in Figure 2.7, the apodization loss is calculated as:

$$\text{Apodization Loss} = -10 \cdot \text{Log}_{10} \left[\frac{(1 + 3 + 5 + 7)^2}{4(1^2 + 3^2 + 5^2 + 7^2)} \right]$$

$$= -10 \cdot \text{Log}_{10} (256/336) = +1.18 \text{ dB}$$

In addition to impacting the amount of insertion loss exhibited by a transducer, apodization also complicates the calculation of

conductance. The conductance of a transducer may be written in terms of the voltage incident on that transducer, V_I, and the power radiated by the transducer, P_r. This relationship is:

$$G_a(f) = P_t/V_I^2 \qquad (2\text{-}13)$$

The power radiated by a transducer must be calculated as the superposition of the power radiated by each channel of the transducer, as was the energy radiated by the transducer. As a result, the conductance of a transducer must be calculated as the superposition of the conductances of each channel.

The conductance of a single tap of the transducer in Figure 2.8 is given by [11]:

$$G_s = 8f_o\, k^2\, C_s\, W_a\, E^2(f) \qquad (2\text{-}14)$$

where:

G_s = conductance of a single tap

f_o = synchronous frequency of the structure

k = acoustic coupling coefficient of the substrate

C_s = the static capacitance of the substrate per unit length of tap

W_a = width of the acoustic beam width

$E(f)$ = the element factor

For the structure shown in Figure 2.8, the synchronous frequency, f_o, is equal to half the sampling frequency, f_s. Therefore, equation (2-14) may be rewritten as:

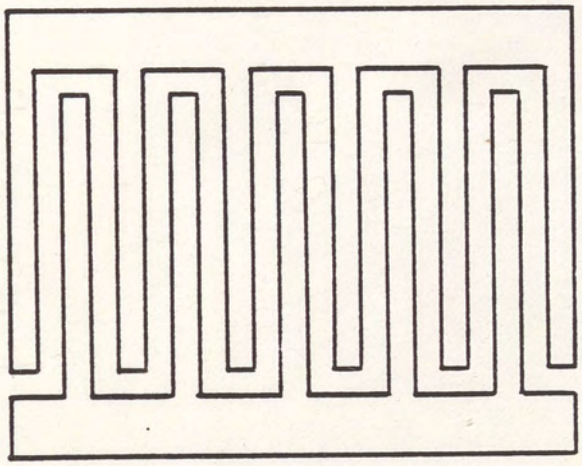

Figure 2.8. Unapodized Transducer.

$$G_s = 4f_s\, k^2\, C_s\, W_a\, E^2(f) \qquad (2\text{-}15)$$

Note that the only frequency dependence of G_s is that of the element factor, E(f). This is because a single tap transducer ideally operates as an impulse function. In the ideal case, where the element factor is excluded, energy is radiated equally over all frequencies. If more than one tap is present in a transducer, it is necessary to calculate the spectral response of the energy transmitted by the transducer in order to calculate the conductance. The energy radiated by a transducer containing "M" unapodized channels was previously stated in equation (2-10). The energy radiated by a transducer is directly related to the power radiated by that transducer. The power radiated is equated to the conductance by

equation (2-13). Therefore, the conductance of a transducer may be calculated from:

$$G_a(f) = G_s \cdot E_t(f) \qquad (2\text{-}16)$$

Substituting G_s and $E_t(f)$ into equation (2-16) from equations (2-15) and (2-10) yields:

$$G_a(f) = 4f_s\, k^2\, C_s\, W_a \cdot E^2(f) \cdot \sum_{i=1}^{M} \frac{1}{M} \cdot |H_i(f)|^2 \qquad (2\text{-}17)$$

For a device sampled at three times the synchronous frequency, $f_s = 3f_o$, the acoustic conductance may be written as:

$$G_a(f) = 12f_o\, k^2\, C_s\, W_a \cdot E^2(f) \cdot \sum_{i=1}^{M} \frac{1}{M} \cdot |H_i(f)|^2 \qquad (2\text{-}18)$$

From the three phase UDT equivalent circuit shown in Figure 2.9, it is apparent that the conductance present at either voltage phase is actually split between the other phase and ground. Therefore, the conductance between any two phases of a three phase device is half that of equation (2-18). The conductance between each pair of phases of a three phase UDT is calculated by SAWCAD2 using:

$$G_{3a}(f) = 6f_o\, k^2\, C_s\, W_a \cdot E^2(f) \cdot \sum_{i=1}^{M} \frac{1}{M} \cdot |H_i(f)|^2 \qquad (2\text{-}19)$$

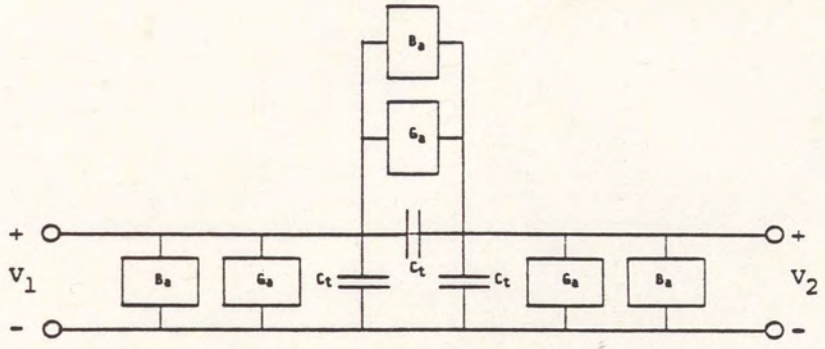

Figure 2.9. Three Phase UDT Equivalent Circuit.

Revisions to SAWCAD2 Menus

No modifications were made to the SAWCAD2 main menu. One additional option was added to the SAWCAD2 analysis menu shown in Figure 2.10. The option is "(E)xamine acoustic electrical effects." The menu driver for this option is shown in Figure 2.11. This menu allows the user to plot the following list of acoustic and electrical quantities.

1. The forward and reverse responses of the transducer.
2. The voltage incident on either of the structures phases, V_1 or V_2.
3. The transducer's acoustic conductance.
4. The transducer's Hilbert transform acoustic susceptance.
5. The element factor.
6. The acoustic energy distribution across the acoustic aperature.
7. The device's reflection coefficient at the input to the network.

```
**************************************************************
*                  <<< SYSTEM DATA STATUS >>>                *
*  LAST INPUT FILE: IMPULSE.DA LAST OUTPUT FILE: undefined   *
*  DATA TYPE: Time             NUMBER OF DATA SAMPLES: 1024  *
*                                                            *
*                   <<< NETWORK STATUS >>>                   *
*         NUMBER OF NODES :  2   SOURCE NODE :  2            *
*  PHASING:  USER DEF NETWORK    MATCHING:  USER DEF NETWORK  *
**************************************************************

              ================================
              <<<     THREE-PHASE UDT      >>>
              <<< A N A L Y S I S  M E N U >>>
              ================================

           (T)ransducer model parameters

           (M)atching/phasing network calculation

           (C)omplete frequency response analysis

           (I)nitialize/reset network elements

           (V)iew network

           (E)xamine acoustic electrical effects

           (Q)uit device analysis

              COMMAND : ==>
```

Figure 2.10. SAWCAD2 Analysis Menu.

```
=====================================
<<<       THREE-PHASE UDT         >>>
<<< EXAMINE ACOUSTICE ARRAY DATA >>>
=====================================

(T)ransducer response, forward or reverse

(N)etwork response, each phase

(C)onductance array data

(S)usceptance array data, acoustic

(E)lement factor data

(B)eam energy profile at fo

(R)eflection coefficient

(Q)uit and return to analysis menu

   COMMAND : ==>
```

Figure 2.11. Examine Acoustic Array Data Menu.

CHAPTER III

REVIEW OF THE THREE PHASE UDT OPERATION

A sample UDT unit cell [12], including the required phasing network, is shown in Figure 3.1. The 60° phase shift network is designed to implement a 60° phase shift in v(t) at the synchronous frequency of the structure, f_o. The synchronous frequency of the structure is defined by:

$$f_o = v_a/\lambda_o \tag{3-1}$$

The term λ_o is the wavelength of one unit cell, as shown in Figure 3.1.

The unidirectional operation of the cell may be understood most easily if the analysis of the UDT structure is limited to its synchronous frequency. The unidirectionality of the device is accomplished in the superposition of the voltage and spatial phases of the cell.

The net wave emerging from a unit cell is the sum of all wave generators.

$$U(w) = \sum_{n=1}^{N} V_n \, e^{j\theta n(w)} \cdot \alpha[e^{-j\phi n(w)} + e^{+j\phi n(w)}] \tag{3-2}$$

where:

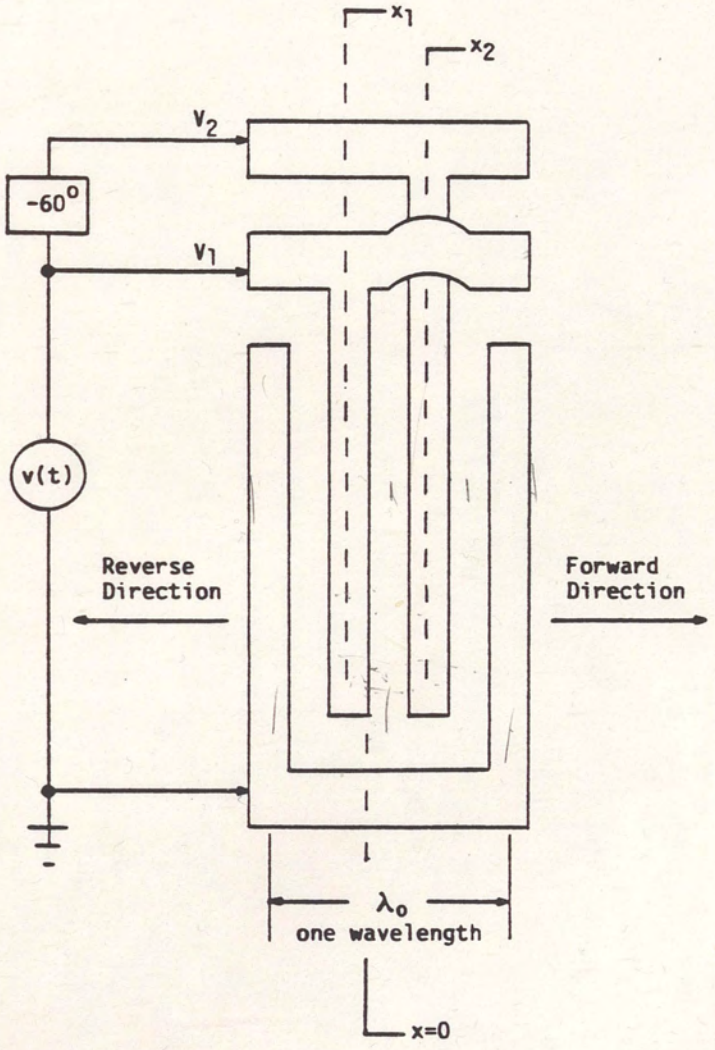

Figure 3.1. Sample Three Phase UDT Unit Cell.

V_n = amplitude of the incident voltage on the generator

θ_n = phase angle of the incident voltage

$\phi_n = -k \cdot x_n$, the spatial phase of the electrode with respect to $x = 0$

$k = 2 \cdot \pi/\lambda$

x_n = the electrode's spatial distance from $x = 0$

α = acoustic wave amplitude constant

The acoustic wave, U(w), is actually the sum of the wave's propagation in the forward and reverse directions.

$$U(w) = U_f(w) + U_r(w) \tag{3-3}$$

$$U_f(w) = \sum_{n=1}^{N} V_n e^{j\theta n(w)} \cdot \alpha e^{-j\phi n(w)} \tag{3-4}$$

$$U_r(w) = \sum_{n=1}^{N} V_n e^{j\theta n(w)} \cdot \alpha e^{+j\phi n(w)} \tag{3-5}$$

From Figure 3.1, at $f = f_o$:

$$x_1 = -\lambda_o/12 \text{ and } x_2 = +\lambda_o/4 \tag{3-6}$$

The voltages, V_1 and V_2, applied to the electrodes are of equal magnitude, but V_2 lags V_1 by 60° at f_o.

$$V_1 = V\underline{/0°} = V \tag{3-7}$$

$$V_2 = V\underline{/-60°} = Ve^{-j\pi/3} \tag{3-8}$$

Therefore, the phases associated with each generator are:

$$\theta_1 = 0 \text{ and } \theta_2 = -\pi/3$$

$$\phi_1 = +\pi/6 \text{ and } \phi_2 = -\pi/2$$

For the wave propagating in the +x direction:

$$U_f(w_o) = V_1 e^{+j\theta 1} \cdot \alpha e^{-j\phi 1} + V_2 e^{+j\theta 2} \cdot \alpha e^{-j\phi 2} \qquad (3\text{-}9)$$

$$= \alpha \cdot V \cdot [e^{j(\theta 1 - \phi 1)} + e^{j(\theta 2 - \phi 2)}]$$

$$= \alpha \cdot V \cdot (e^{-j\pi/6} + e^{j\pi/6})$$

$$= \alpha \cdot V \cdot 2 \cdot \cos(\pi/6)$$

$$= \alpha \cdot V \cdot \sqrt{3}$$

For the wave propagation in the -x direction:

$$U_r(w_o) = V_1 e^{+j\theta 1} \cdot \alpha e^{+j\phi 1} + V_2 e^{+j\theta 2} \cdot \alpha e^{+j\phi 2} \qquad (3\text{-}10)$$

$$= \alpha \cdot V \cdot [e^{j(\theta 1 + \phi 1)} + e^{j(\theta 2 + \phi 2)}]$$

$$= \alpha \cdot V \cdot (e^{j\pi/6} + e^{-j5\pi/6})$$

$$= \alpha \cdot V \cdot (1 + e^{-j\pi}) \, e^{j\pi/6}$$

$$= 0$$

The phasor analysis of the forward and reverse wave propagation may also be represented graphically as in Figure 3.2(a) and (b), respectively [13].

The phasor analysis presented is only valid at f_o. As frequency deviates from f_o, the spatial phases, $\phi_n(w)$, will rotate and the voltage phasor, θ_2, deviates from 60°. The result is that power begins to radiate in the reverse direction. Although this does impact the unidirectional bandwidth of the device, forward to reverse power flow ratios, defined by:

$$\text{Power Flow Ratio} = 20 \cdot \text{Log}_{10}|[\, U_f(w)|/|U_r(w)|] \qquad (3\text{-}11)$$

of greater than 20 dB have been attained [1] for fractional bandwidths of 20%.

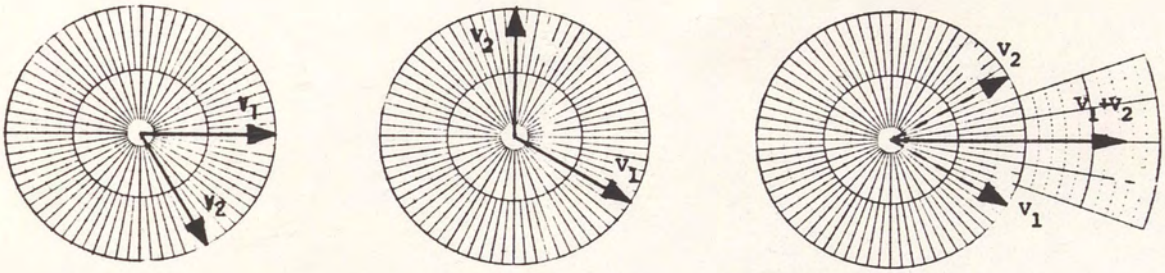

Voltage Phase | Spatial Phase | Resultant Phase

Figure 3.2(a). Forward Phasor Relationships.

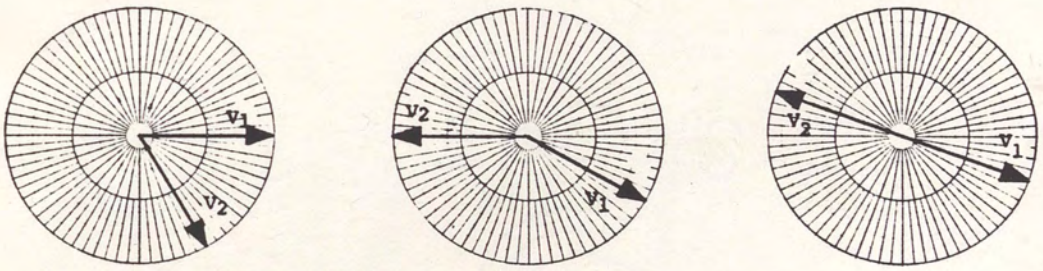

Voltage Phase | Spatial Phase | Resultant Phase

Figure 3.2(b). Reverse Phasor Relationships.

CHAPTER IV

GUIDELINES FOR THE APODIZATION OF UDTs

In order to develop a sufficient apodization structure for UDTs, all restrictions and guidelines must first be stated for such a structure. As noted earlier, for a given cell, the tap lengths of each phase must be of equal length and colinear for unidirectional power flow to occur along the entire length of each tap. By superposition of cells of varying tap lengths, it becomes evident that the ideal impulse response of each phase, $h_1(t)$ and $h_2(t)$, must satisfy:

$$h_2(t) = h_1(t - t_o/3) \tag{4-1}$$

Here, t_o is equal to the time required for an acoustic signal to travel one wavelength along the acoustic substrate. The relationship stated in equation (4-1) is illustrated graphically in Figure 4.1(b).

The forward acoustic response, U_f, of a unidirectional transducer may be described as a sum of the convolutions of the voltage phases and their respective impulse responses as:

$$U_f = V_1(t) * h_1(t) + V_2(t) * h_2(t) \tag{4-2}$$

Substituting $h_1(t) = h(t)$ and $h_2(t) = h(t - t_o/3)$:

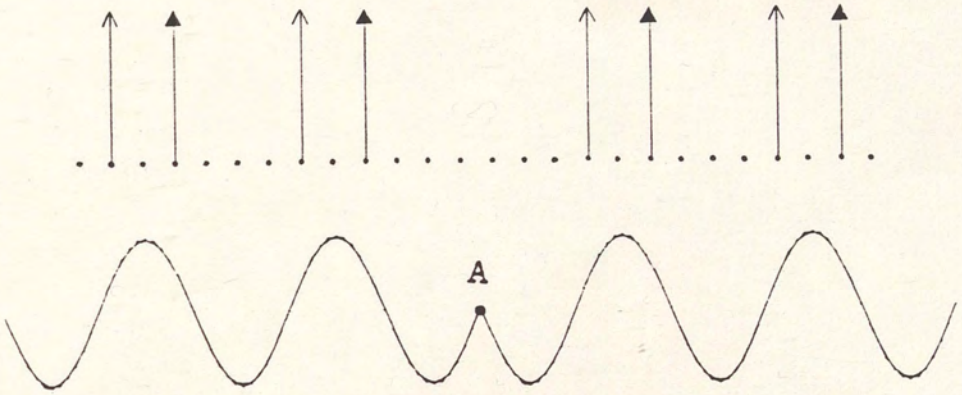

Figure 4.1(a). Impulse Response $h_1(t) + h_2(t)$. In addition to the impulse responses of $h_1(t)$ and $h_2(t)$, the synchronous signal of the impulse response is shown. There is a phase reversal at point "A" similar to that occurring in a time sidelobe.

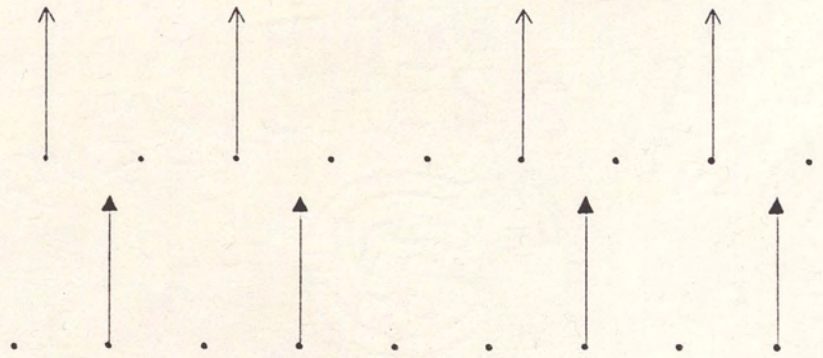

Figure 4.1(b). Impulse Responses $h_1(t)$ and $h_2(t)$.

$$U_f = V_1(t) * h(t) + V_2(t) * h(t - t_o/3) \qquad (4\text{-}3)$$

An arbitrary finite impulse response h(t) may be defined as:

$$h(t) = \sum_{n=1}^{N} a_n \cdot \delta(t - t_n) \qquad (4\text{-}4)$$

Three restrictions shall be applied to h(t). First, due to the nature of the array factor, each relative tap magnitude, a_n, must be non-negative [14]. However, an effective negative tap may be implemented by spatially phasing the tap. Such a spatial phase change is implemented by placing the unit cell an additional half wavelength, $\lambda_o/2$, from the last unit cell. This spatial delay of $\lambda_o/2$ is equivalent to a delay in time of $t_o/2$ or a phase of 180 degrees at the synchronous frequency, f_o. Such a spatial phase change is illustrated by the impulse response shown in Figure 4.1(a). The impulse response in Figure 4.1(a) is accompanied by the effective response of the array at the synchronous frequency, f_o.

The second restriction is, given that each cell occupies one wavelength, all unit cells must be spatially separated by at least one wavelength. This requires that:

$$t_o \leq t_{n+1} - t_n; \text{ for } 0 < n < N \qquad (4\text{-}5)$$

The third restriction on h(t) is that the greatest common factor, GCF, of all t_n shall be limited to $t_o/2$. The resulting requirement on all t_n is:

$$t_n = m \cdot t_o/2, \text{ for m an arbitrary integer} \qquad (4\text{-}6)$$

The validity of choosing a GCF of $t_o/2$ is illustrated by Figure 4.1 as the sum of $h_1(t)$ and $h_2(t)$ for an unweighted impulse response; the GCF is $t_o/6$. However, as stated in equation (4-2), the acoustic response of the transducer is defined as the sum of the products of each voltage phase with its corresponding impulse response. Therefore, by extracting each phase's impulse response from Figure 4.1(a), as shown in Figure 4.1(b), the GCF of the impulse response becomes $t_o/2$.

CHAPTER V

GENERATION OF A UDT APODIZATION STRUCTURE

In generating an apodized UDT, an ideal impulse response and its array factor is required as shown in Figure 5.1(a) and (b), respectively. Note that all restrictions on the array factor outlined earlier are met by the array factor in Figure 5.1(b). Next, a cell for each tap must be generated and combined through superposition to generate a structure as shown in Figure 5.2. The bus bars and crossovers are not illustrated in Figure 5.2 in order to simplify the figure.

The structure depicted in Figure 5.2 has some problems associated with it. First, since all taps are aligned to the same side of the transducer, the majority of the acoustic energy is concentrated on one side of the beam, resulting in a non-uniform energy distribution across the beam. Such non-uniform energy distributions can result in excessive apodization loss and passband distortions. A second problem is that the structure is not balanced. Due to the required crossovers, the capacitance between the phases V_1 and V_2 is not the same as that between either phase and ground. This is illustrated in Figure 5.3. The network components in Figure 5.3 are defined as:

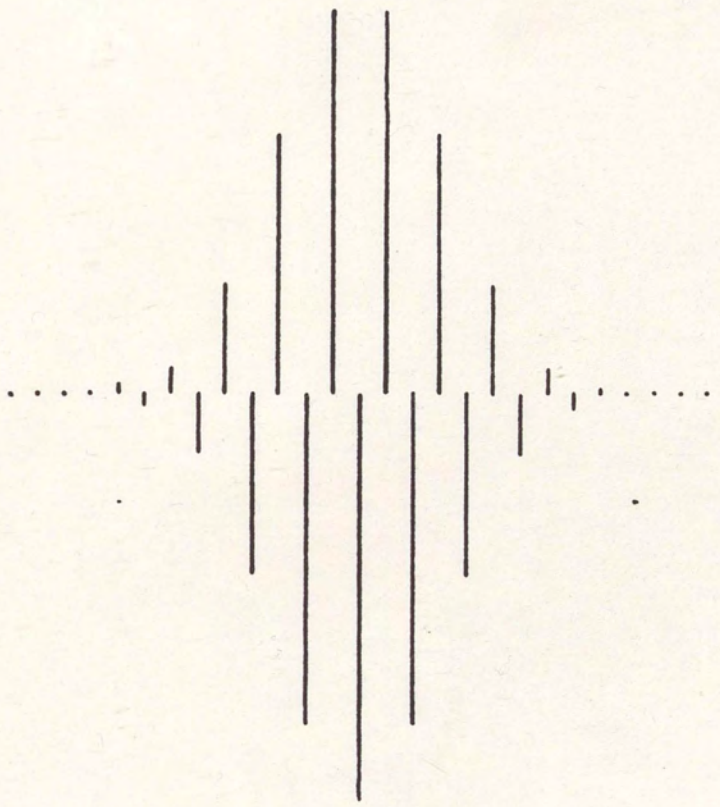

Figure 5.1(a). Sample Impulse Response.

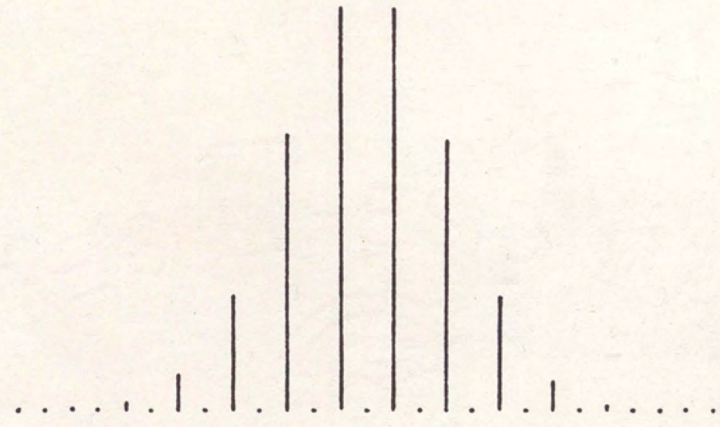

Figure 5.1(b). Sample Array Factor.

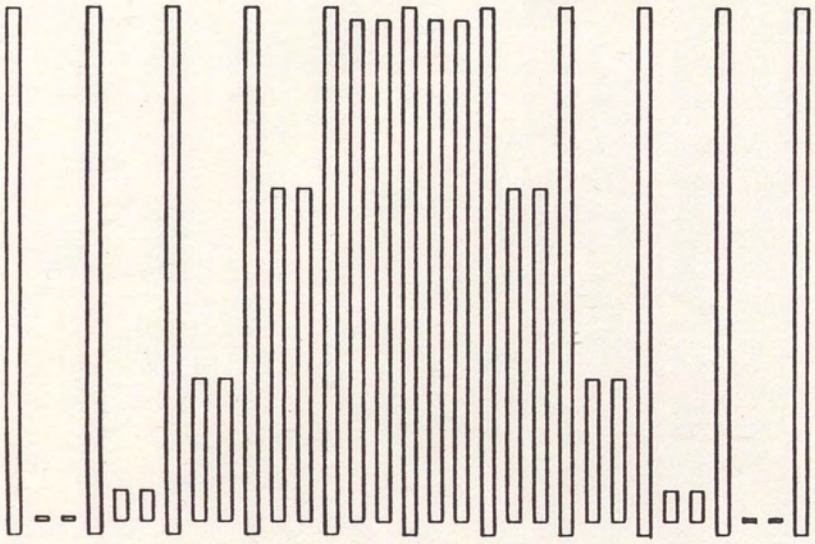

Figure 5.2. Apodized UDT Electrode Arrangement. The bus bars and crossovers are not shown.

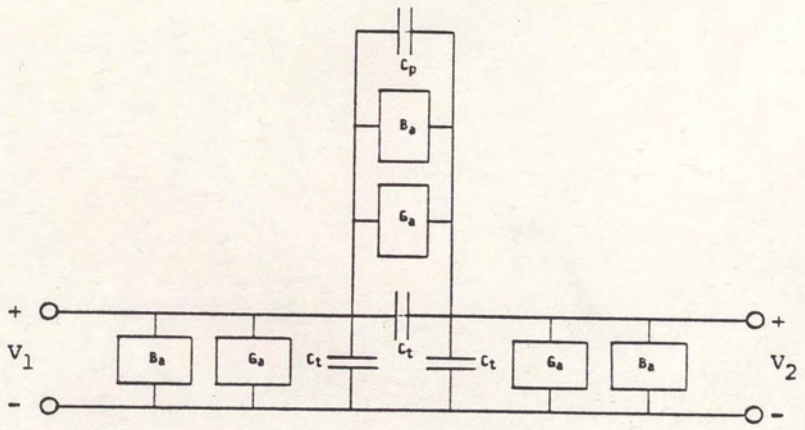

Figure 5.3. Unbalanced UDT Equivalent Circuit.

G_a = Acoustic Conductance

B_a = Hilbert Transform Acoustic Susceptance

C_t = Transducer Static Capacitance

C_p = Transducer Parasitic Capacitance

G_a, B_a and C_t are all the result of interactions between the electrodes of the transducer. C_p is the result of the parasitic capacitances of the crossovers shown in Figure 5.2(a).

The shortfalls of the unbalanced structure may be compensated for through increased complexity of the structure. First, a cell may be developed for which the capacitances due to crossovers are balanced between all three phases. Such a cell is shown in Figure 5.4(a). The equivalent circuit of this balanced structure is illustrated in Figure 5.4(b). Note that, to achieve a balanced structure, twice as many crossovers must now be constructed.

In order to fully compensate for the non-uniform beam profile, it would be necessary to place each tap at arbitrary positions across the acoustic beam. However, this is not possible. Each tap must be aligned to an edge of the acoustic beam. A compromise is to align taps arbitrarily to either side of the acoustic beam. If the impulse response of the UDT is not dispersive, then the beam profile may be made most uniform by aligning the even taps to one side of the beam and the odd taps to the other side of the beam [15]. A simple illustration of how this may be accomplished is given in

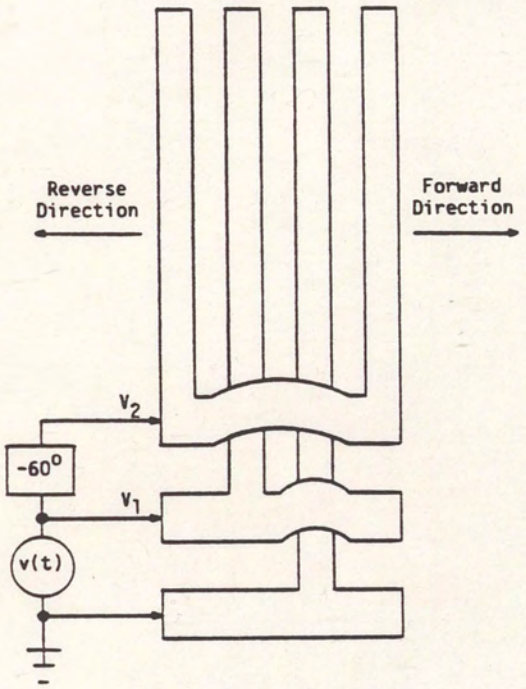

Figure 5.4(a). Balanced UDT Unit Cell.

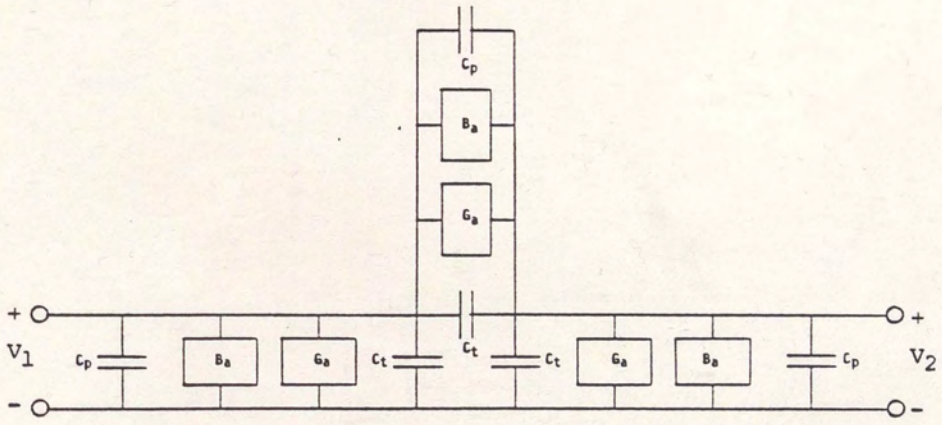

Figure 5.4(b). Balanced UDT Equivalent Circuit.

Figure 5.5, for a series of unweighted UDT cells. An example implementing the same array factor as the unbalanced structure in Figure 5.2 is shown in Figure 5.6.

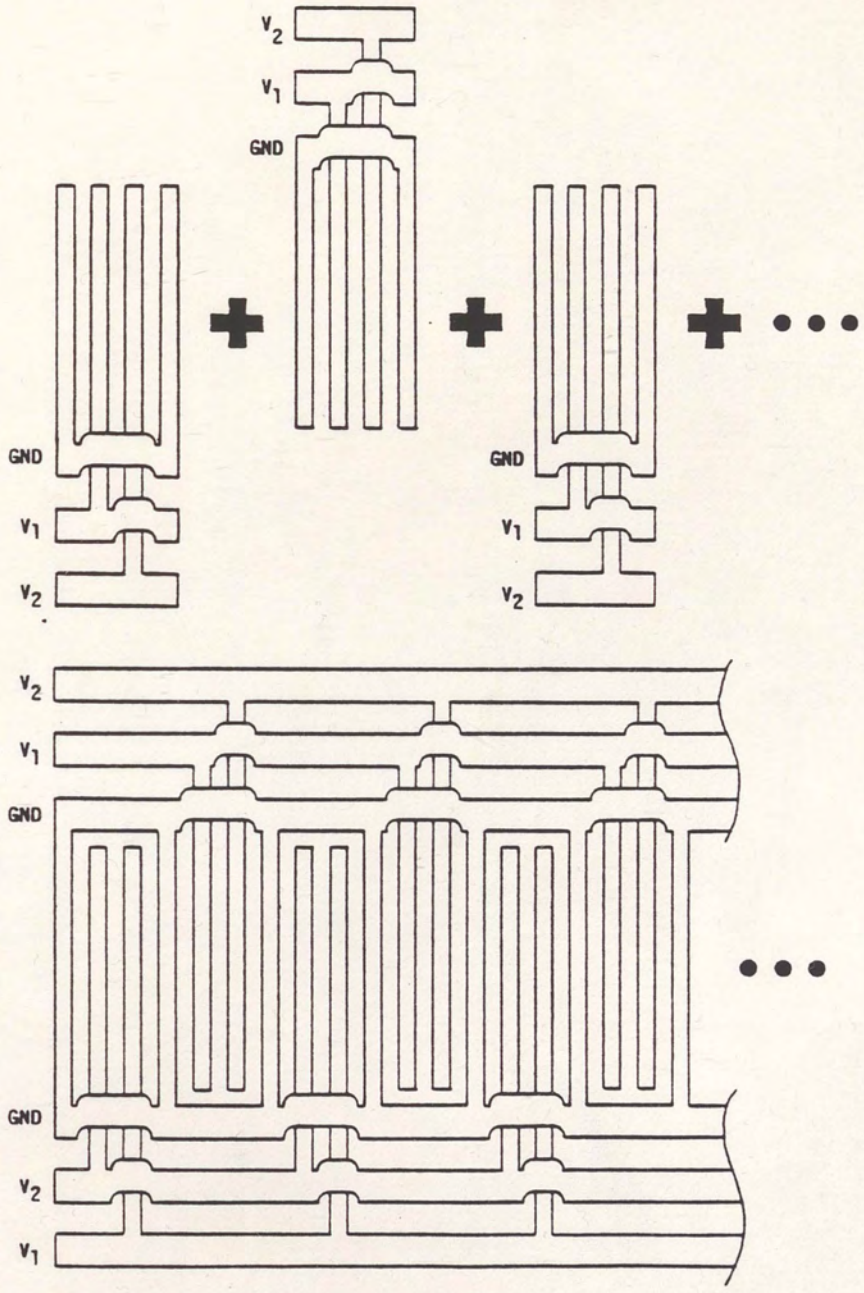

Figure 5.5. Superposition of Unit Cells.

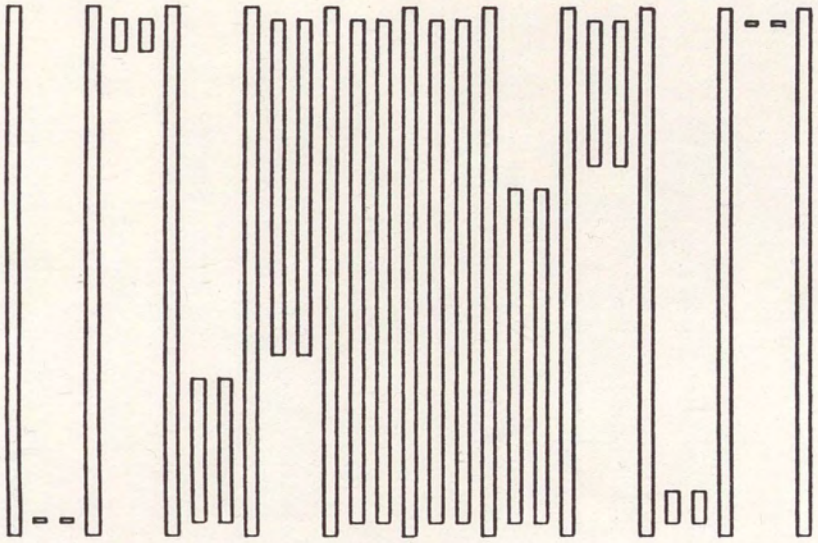

Figure 5.6. Balanced UDT Electrode Arrangement. The bus bars and crossovers are not shown.

CHAPTER VI

COMPARISON OF THE STRUCTURES

Through the use of an example, the effects of the two structures may be compared. The impulse response in Figure 6.1(a) was generated by SAWCAD2 [9] using eigen synthesis [16]. The array factor of a single phase is shown in Figure 6.1(b). The ideal frequency response and array factor responses are shown in figures 6.2(a) and 6.2(b), respectively. The array factor response will be used as a reference when examining the effects of the two apodization structures. The narrow band array factor response is shown in Figure 6.3. Note that the passband ripple of the array factor response is less than 0.02 dB.

SAWCAD2 has been updated to perform transducer analysis by splitting the transducer into channels [17] and analyzing the acoustic response of each channel. The complete response is given as the superposition of all the channels.

The acoustic energy distributions across the beam of each transducer structure are shown in figures 6.4(a) and 6.4(b). It is readily apparent that the balanced structure has a significantly more uniform energy profile. The apodization losses of the balanced and unbalanced structures are 0.283 and 0.659 dB, respectively. The acoustic conductance and Hilbert transform susceptance, as

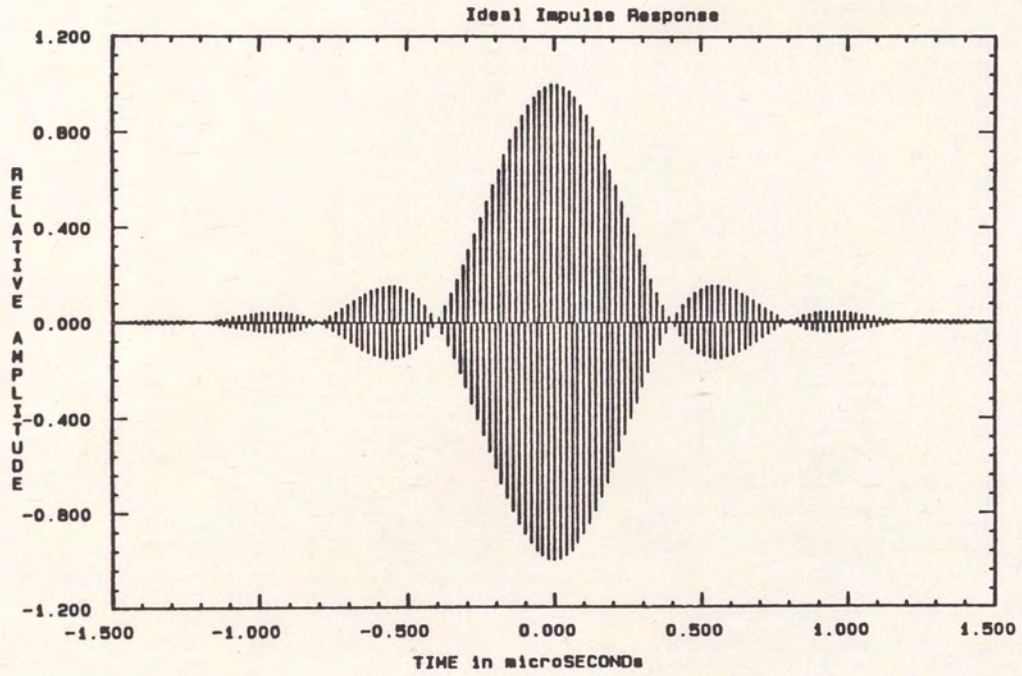

Figure 6.1(a). Impulse Response Generated by SAWCAD2.

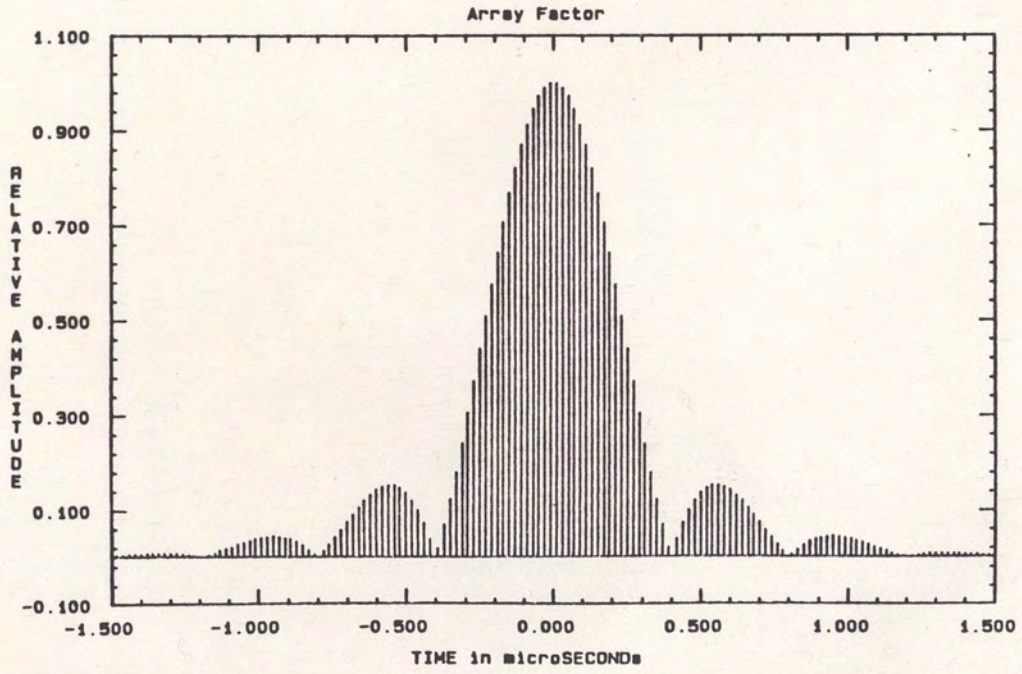

Figure 6.1(b). Array Factor Generated by SAWCAD2.

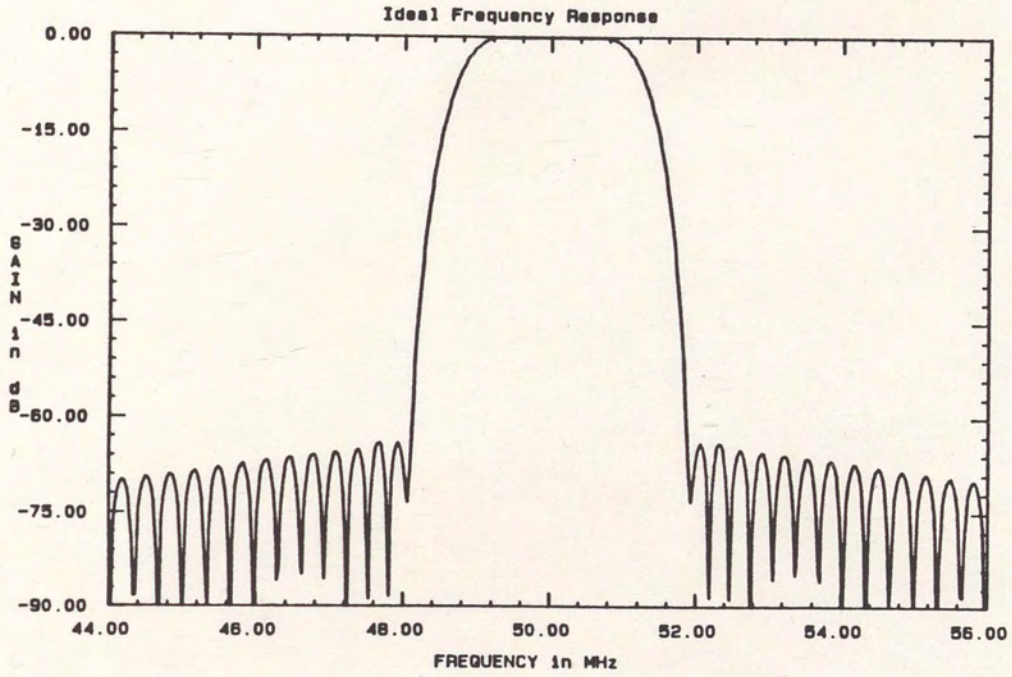

Figure 6.2(a). Ideal Frequency Response.

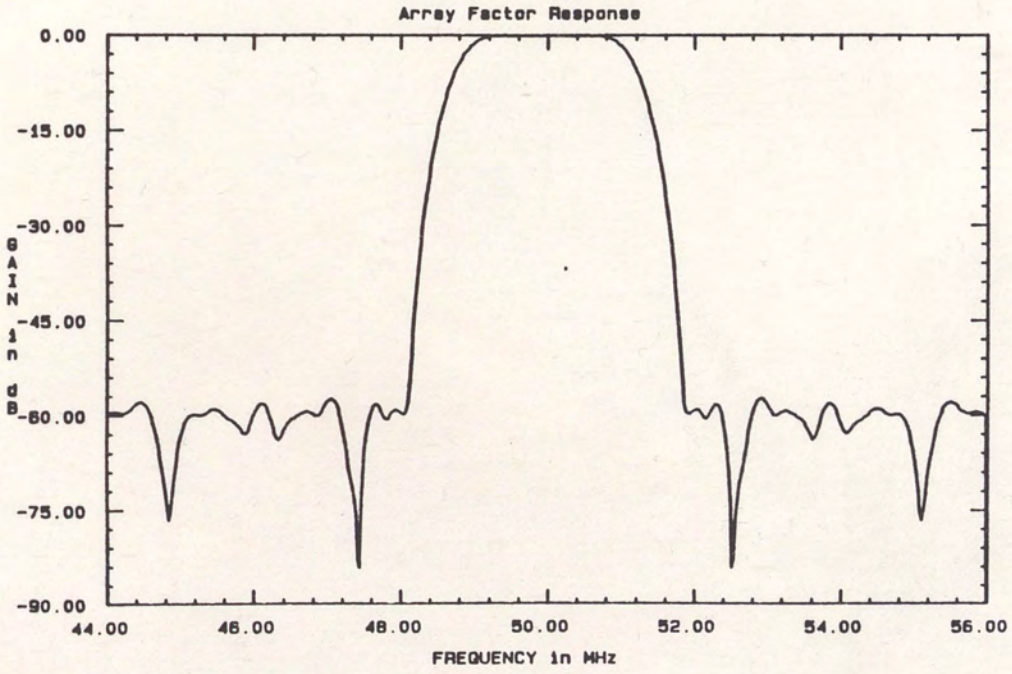

Figure 6.2(b). Array Factor Wideband Response.

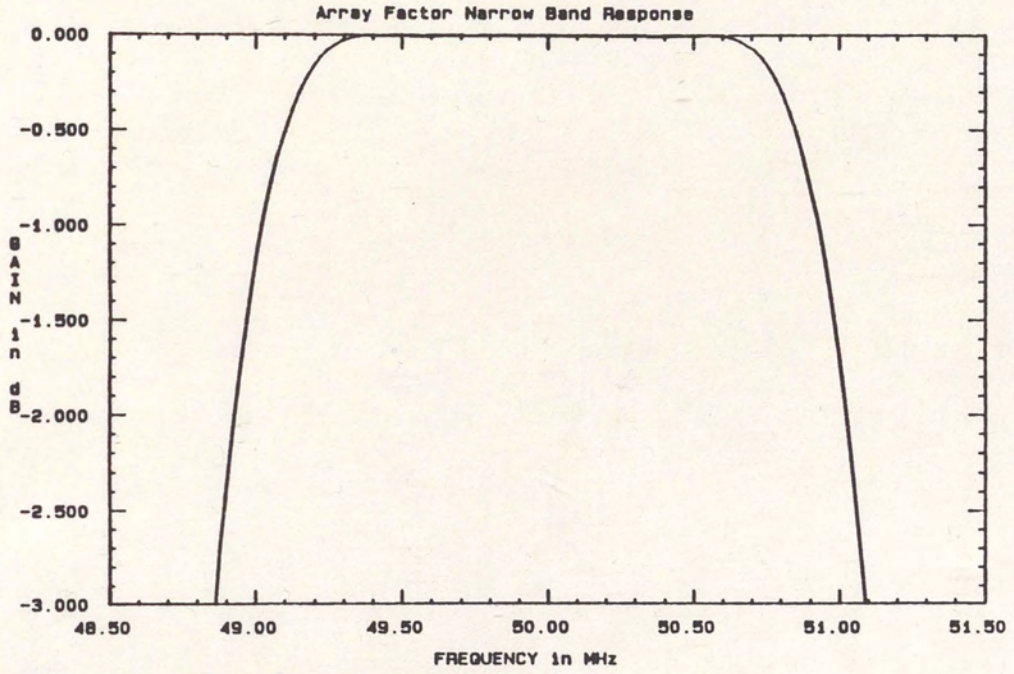

Figure 6.3. Array Factor Narrowband Response.

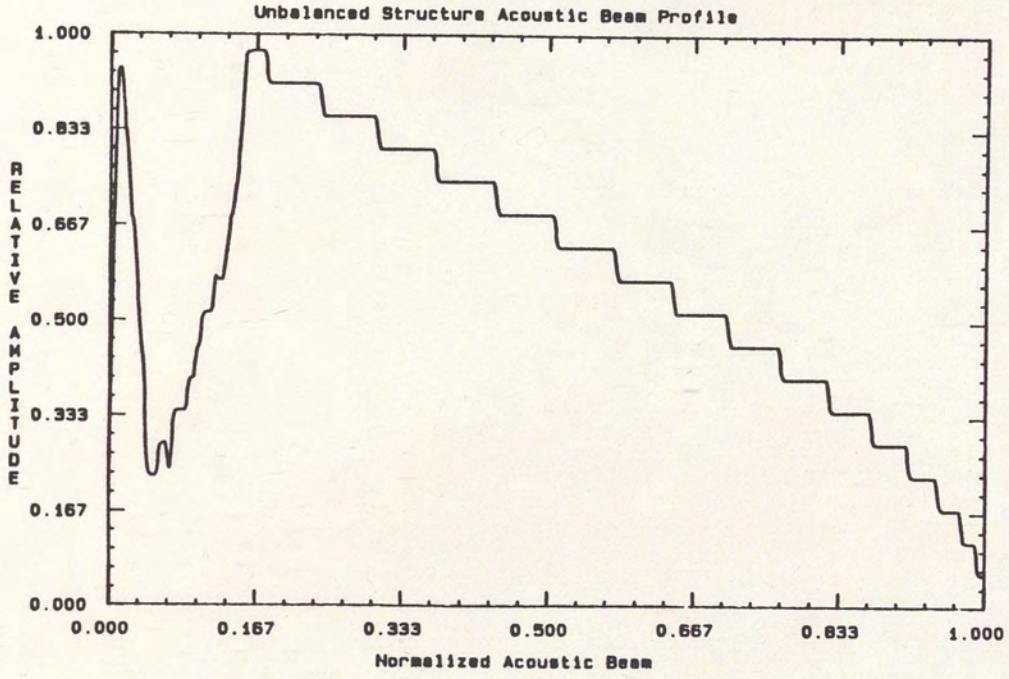

Figure 6.4(a). Unbalanced Structure Energy Distribution. Radiated energy is plotted versus its position across the acoustic aperature.

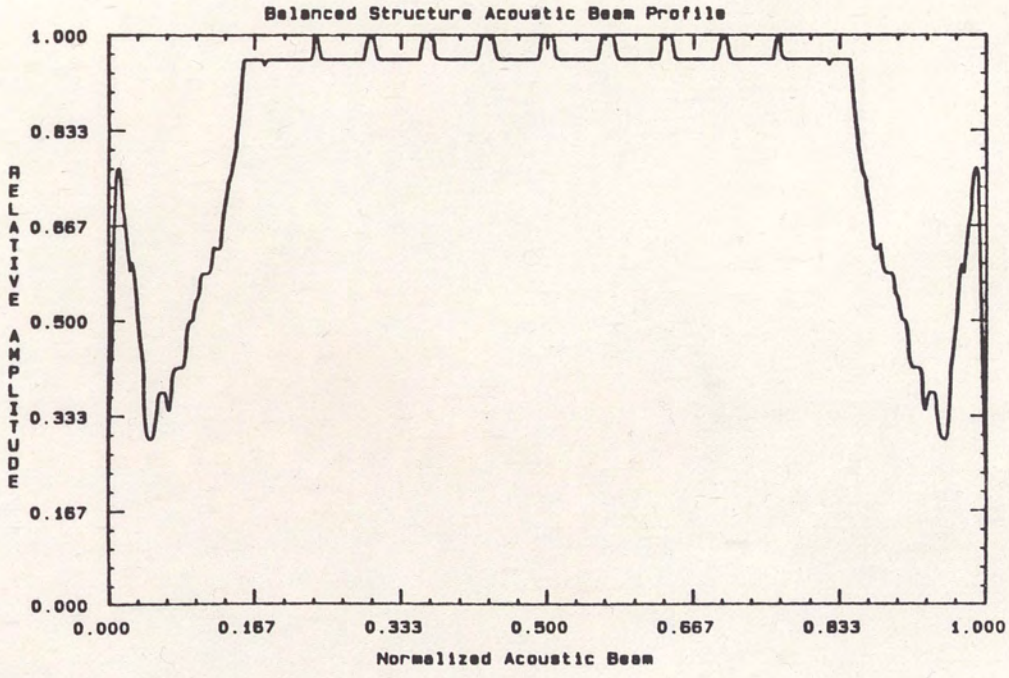

Figure 6.4(b). Balanced Structure Energy Distribution. Radiated energy is plotted versus its position across the acoustic aperature.

predicted by SAWCAD2, are shown in figures 6.5(a), 6.5(b), 6.6(b) and 6.6(b). Note that the conductance of the balanced structure exhibits significantly less ripple than that of the unbalanced structure. The slant of the conductance results from the element factor [10].

Performing an electrical network analysis of the two structures using SAWCAD2 under phased and matched conditions results in the forward responses in figures 6.7(a) and 6.7(b). The frequency responses of the two structures are noticeably different. The response of the unbalanced structure exhibits significantly more passband distortion than the balanced structure. This is more apparent in the narrowband responses shown in figures 6.8(a) and 6.8(b). In addition to apodization losses, the effects of slight mismatch loss and thin film resistive losses are apparent in the narrow band responses.

Note that there is an obvious correlation between passband ripple and ripple in the acoustic conductance. The acoustic conductance of the balanced structure peaks once and, as a result, its frequency response dips once. The acoustic conductance of the unbalanced structure peaks three times and, as a result, its frequency response dips three times.

It is obvious that the balanced structure is superior to the unbalanced structure using the insertion loss and passband distortion as criteria for comparison.

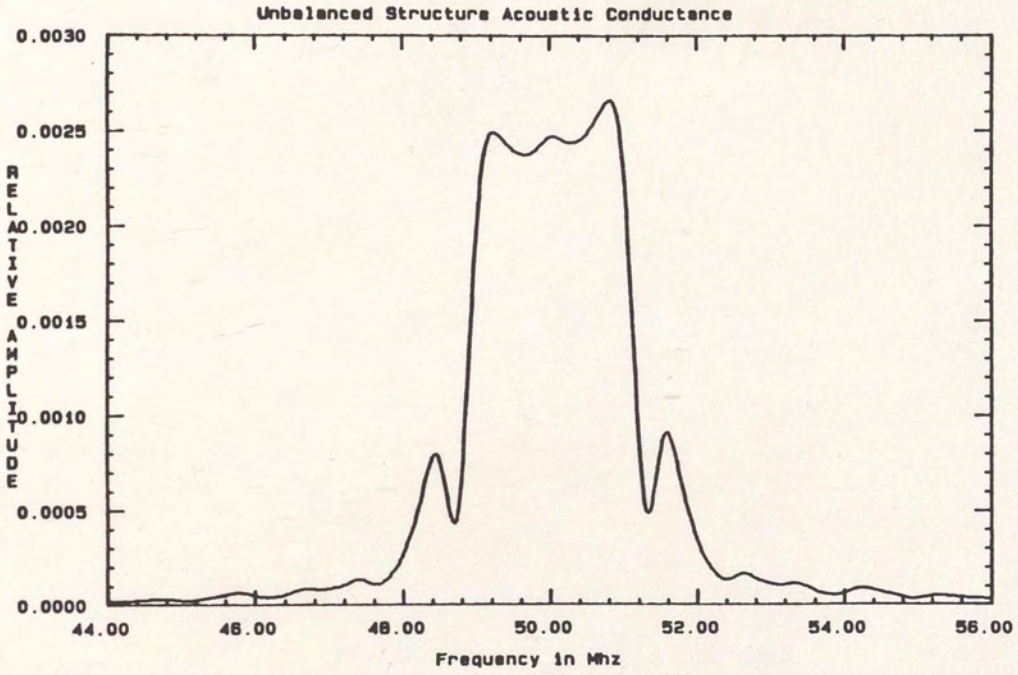

Figure 6.5(a). Unbalanced Structure Acoustic Conductance.

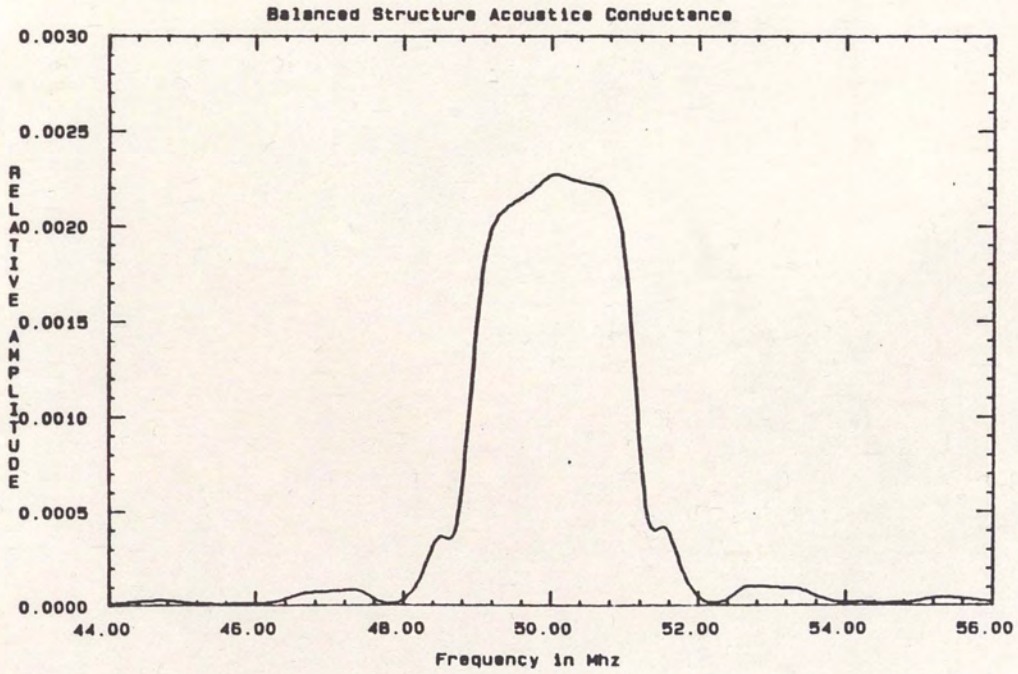

Figure 6.5(b). Balanced Structure Acoustic Conductance.

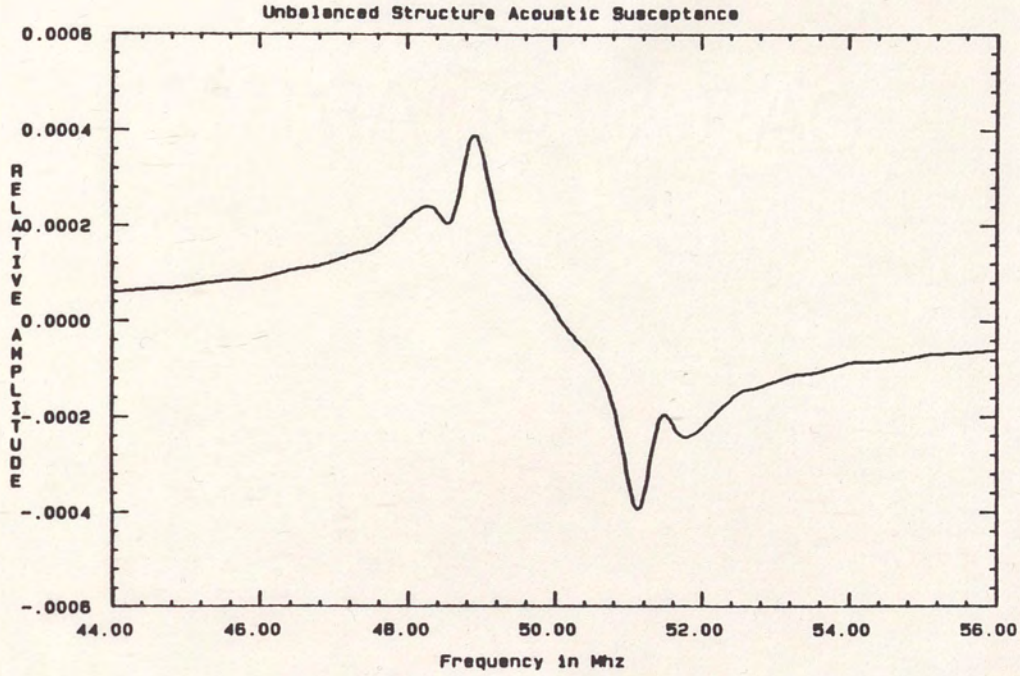

Figure 6.6(a). Unbalanced Structure Hilbert Transform Susceptance.

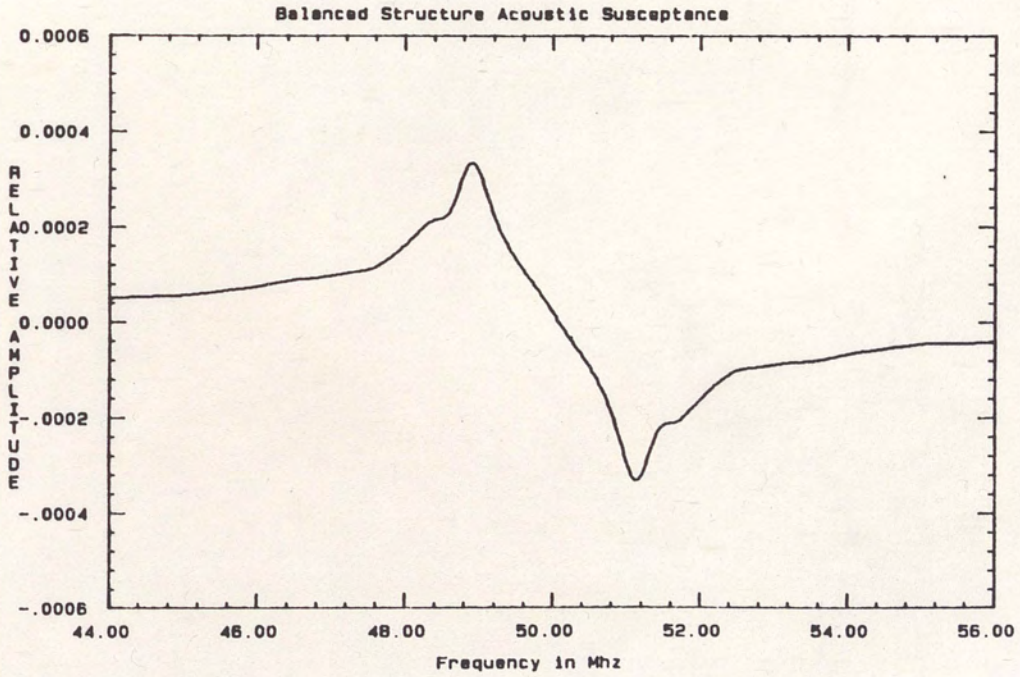

Figure 6.6(b). Balanced Structure Hilbert Transform Susceptance.

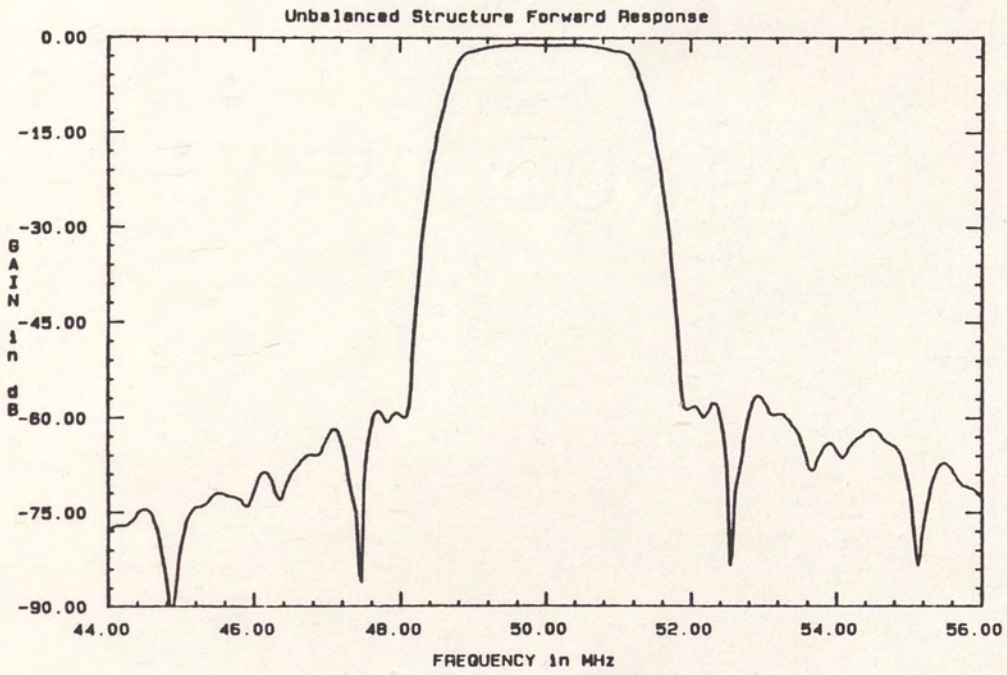

Figure 6.7(a). Unbalanced Structure Wideband Forward Frequency Response.

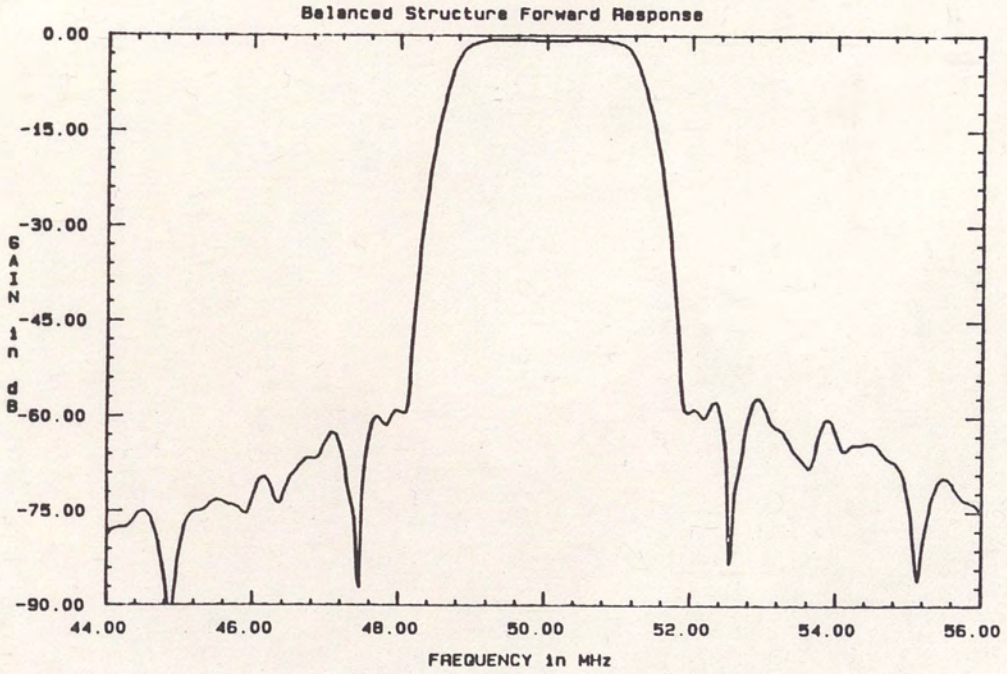

Figure 6.7(b). Balanced Structure Wideband Forward Frequency Response.

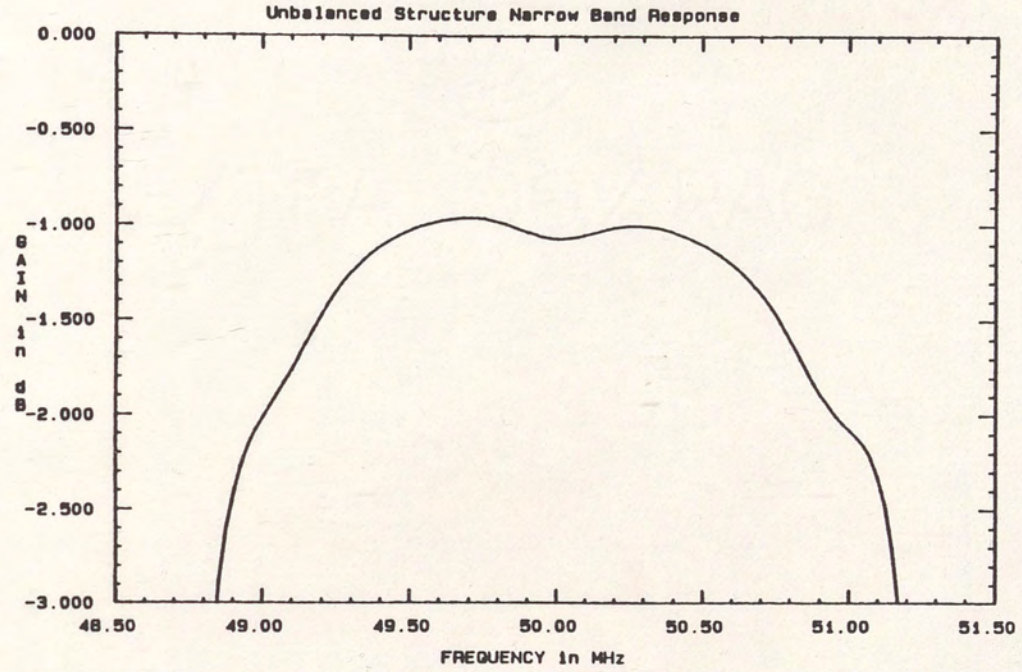

Figure 6.8(a). Unbalanced Structure Narrowband Frequency Response.

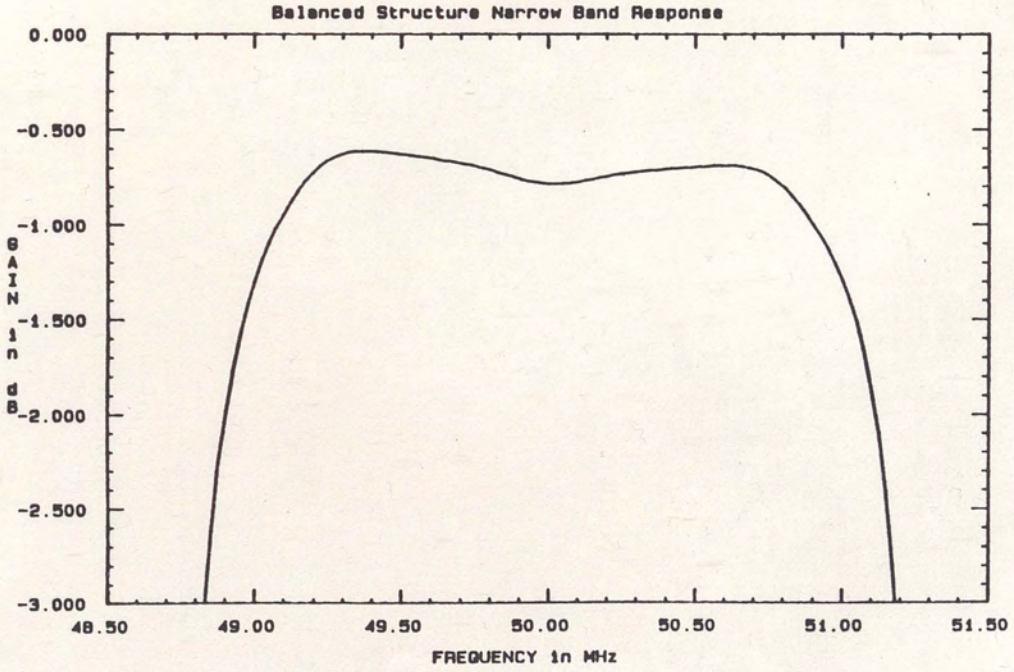

Figure 6.8(b). Balanced Structure Narrowband Frequency Response.

Although no information contributing to the comparison of the two structures is given, the reverse responses of the two structures is illustrated in figures 6.9(a) and 6.9(b). It is apparent from these figures that the transducers maintain a large degree of unidirectionality over their entire bandwidths (fractional bandwidth is 5%).

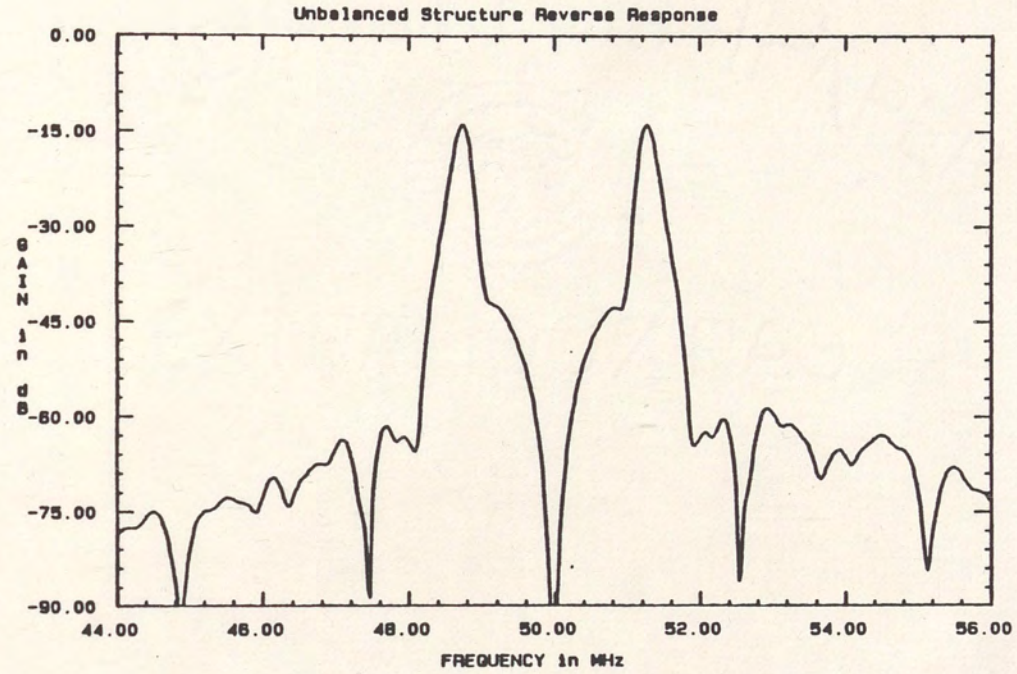

Figure 6.9(a). Unbalanced Structure Reverse Frequency Response.

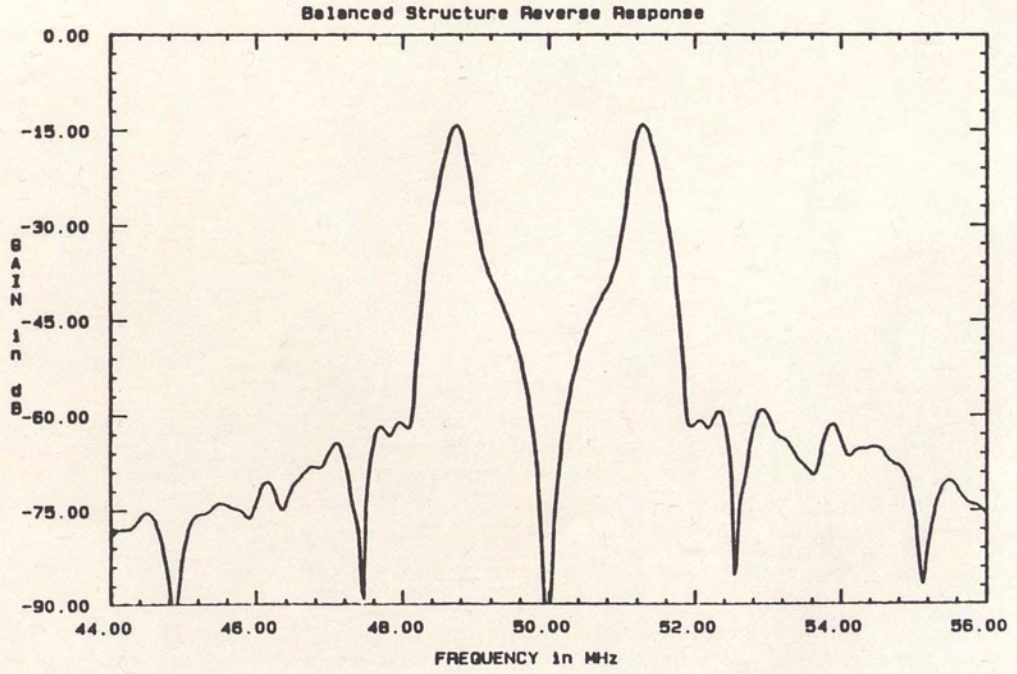

Figure 6.9(b). Balanced Structure Reverse Frequency Response.

CHAPTER VII

STRUCTURAL IMPLEMENTATION

Summary of STRUCTURE2

To compliment the SAWCAD2 analysis program, a FORTRAN-77 program was written for the purpose of generating the masks required for the fabrication of a three phase UDT balanced structure. This program shall be referred to as STRUCTURE2.

STRUCTURE2 was written to allow the user as much flexibility as possible in selecting the geometries necessary in generating a three phase UDT. STRUCTURE2 allows the user to arbitrarily specify the dimensions for the bus bar height, the acoustic beamwidth/ aperature, the electrode to bus bar gap, the electrode finger width, the electrode gap, the electrode-dummy break distance, bond pad width and height, the crossover pad width and height and the via hole width and height. In addition to the automatic generation of transducer structures, STRUCTURE2 allows for manual manipulation of the structures. Rectangles may be manually specified by the user for addition or deletion from the structure. The structures generated may also be scaled and shifted arbitrarily. To aid in the design of SAW device structures, STRUCTURE2 allows the user to graphically view the rectangles. The graphics driver supports Tektronix 4XXX type terminals. The graphics driver allows the user to zoom in and

out on a structure in addition to translating the view port or arbitrarily redefining the view port.

The main menu to STRUCTURE2 is shown in Figure 7.1. Each option is outlined below.

1. (S)tructure Parameters View/Modify: Allows the user to redefine the geometrical parameters which STRUCTURE2 uses when generating a transducer from time impulse response data. When this option is selected, the menu in Figure 7.2 will be displayed. The user will then have a chance to accept or modify the parameters displayed.

2. (M)odify Structure Manually: Allows the user to manually add rectangles to the structure. The user will be prompted for the coordinates of the lower lefthand corner of the rectangle, the width and height of the rectangle, the angle (in degrees) the rectangle is to be rotated counter-clockwise about the lower lefthand corner, the number of rectangles to be generated by the previous definitions and, finally, if more than one rectangle is to be generated. Then the user is prompted for the distance in x and y between rectangles.

3. (C)reate Transducer Geometry: This option automatically generates the three mask levels necessary for the fabrication of a three phase UDT. In order to select this option, time impulse response data must be present in the system. The time impulse response data must be sampled at twice the synchronous frequency of

```
<<< STRUCTURE MAIN MENU >>>

(S)tructure parameters view/modify
(M)odify structure manually
(C)reate transducer geometry
(G)raph structure
(W)rite data to disk
(R)ead data from disk
(F)ile information & modification
(E)rase all file data
(Q)uit - end structure session

COMMAND : ==>
```

Figure 7.1. STRUCTURE2 Main Menu.

```
<<< Transducer Geometry Parameters  >>>
<<< ALL units are in fo wavelengths >>>

starting (X,Y) coordinates ---- : 0.0000E+00, 0.0000E+00
bus bar height ---------------- :  1.500
acoustic beamwidth/aperature -- :  50.00
electrode to bus bar gap ------ : 0.5000
finger width ------------------ : 0.1667
electrode gap ----------------- :  1.000
electrode-dummy break distance  : 0.3333
bond pad width ---------------- :  5.000
bond pad height --------------- :  5.000
bridge pad width -------------- : 0.6000
bridge pad height ------------- : 0.6000
via hole width ---------------- : 0.5000
via hole height --------------- : 0.5000

   OPTIONS  :  (A)ccept values - return to main menu
               (M)odify geometry parameters

   ENTER OPTION : ==>
```

Figure 7.2. Geometrical Parameters Menu.

the device, $2 \cdot f_o$. As STRUCTURE2 generates each mask, the program outputs each mask to the mass storage device. The user will be given a chance to specify the name of the file containing each mask. When all masks have been generated, STRUCTURE2 will display rectangle information such as that shown in Figure 7.3. STRUCTURE2 will then return the user to the main menu with all three masks still in the system. A graphical display of these masks will show them superimposed on each other.

4. (G)raph Structure: Allows the user to visually view the structure on a Tektronix 4XXX compatible terminal. The graphics driver for this option allows the user to zoom in and out on the structure in addition to translating or redefining the view port.

5. (W)rite Data to Disk: Allows the user to output all file information present in the system to the mass storage device, generally a large capacity hard disk.

6. (R)ead Data from Disk: Allows the user to input file information to the system. Either impulse response data or structural data may be read into the system from the mass storage device.

7. (F)ile Information and Modification: Selecting this option will result in the menu in Figure 7.4 being displayed. Viewing the file information will result in data such as that in Figure 7.3 being displayed. The second option of this menu allows the user to rescale and/or shift the rectangles present in the system. This menu

```
 << Structure Files Information >>
 Reference for data is LLHC
**** ITOTAL=  134 ******************

File# 1: ILO=   1 IHI= 116


file-x:min,max=(  -4.0000   16.0000)
file-y:min,max=( -12.5000   16.2000)
width: min,max=(   0.1507   13.0000)
height:min,max=(   0.0800   10.6000)
    arithmetic
        center=(   6.0000    1.8500)

File# 2: ILO= 117 IHI= 132


file-x:min,max=(  -3.7500   15.7500)
file-y:min,max=(  -7.8500    7.8500)
width: min,max=(   0.5000    0.5000)
height:min,max=(   0.7000    0.7000)
    arithmetic
        center=(   6.0000    0.0000)

File# 3: ILO= 133 IHI= 134


file-x:min,max=(  -4.0000   16.0000)
file-y:min,max=(  -8.0000    8.0000)
width: min,max=(  16.5000   16.5000)
height:min,max=(   1.0000    1.0000)
    arithmetic
        center=(   6.0000    0.0000)

Enter return to continue >
```

Figure 7.3. Rectangle Information.

```
        << Modify File Structure Menu >>

(V)iew File Information
(S)cale and/or (S)hift Rectangles
(D)elete a file from structure
(Q)uit and return to Main Menu
        Command ==>
```

Figure 7.4. File Information and Modification Menu.

also allows the user to delete entire structure files. STRUCTURE2 is able to do this since it keeps track of each file separately. Therefore, if two structure files were read into the system, the first could be deleted without altering the rectangles defined by the second.

8. (E)rase All File Data: This option erases all file data from the system. This option is used to initialize STRUCTURE2.

A Sample UDT Structure

STRUCTURE2 generates three mask levels. Figure 7.5 shows a sample of the mask levels of an unapodized transducer superimposed on each other. Each of the three individual mask levels are illustrated in figures 7.6(a), 7.7 and 7.8, respectively.

The first mask level is used to generate the electrode pattern and crossover pads. The crossover pads may be thought of as columns required to hold up a bridge. The second mask level is used to open the via holes in the dielectric so that the crossovers may make contact with the pads. The third mask level is used to generate the crossovers.

Notice that the electrodes in Figure 7.6(b) span out away from each other at the edge of the beam. This is to minimize the radiation of acoustic energy outside the acoustic beam. The amount of rectangle overlap is minimized on the first mask level to reduce "blooming" of the rectangles which can occur when generating the mask using an E-beam machine. The rectangle overlap of Figure 7.6(a) is shown magnified in Figure 7.6(c).

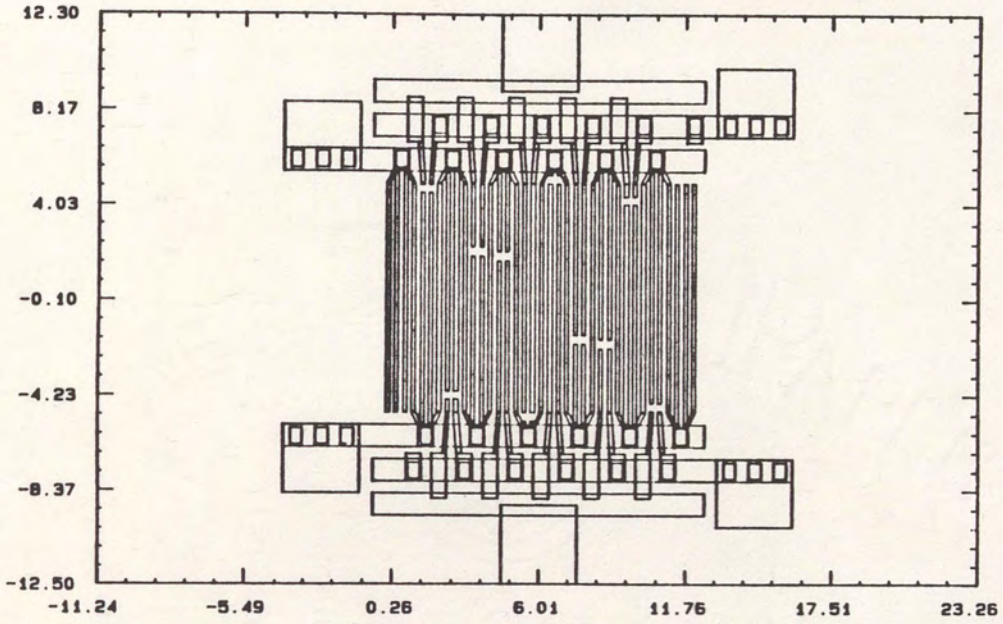

Figure 7.5(a). Sample Apodized UDT, All Mask Levels Shown.

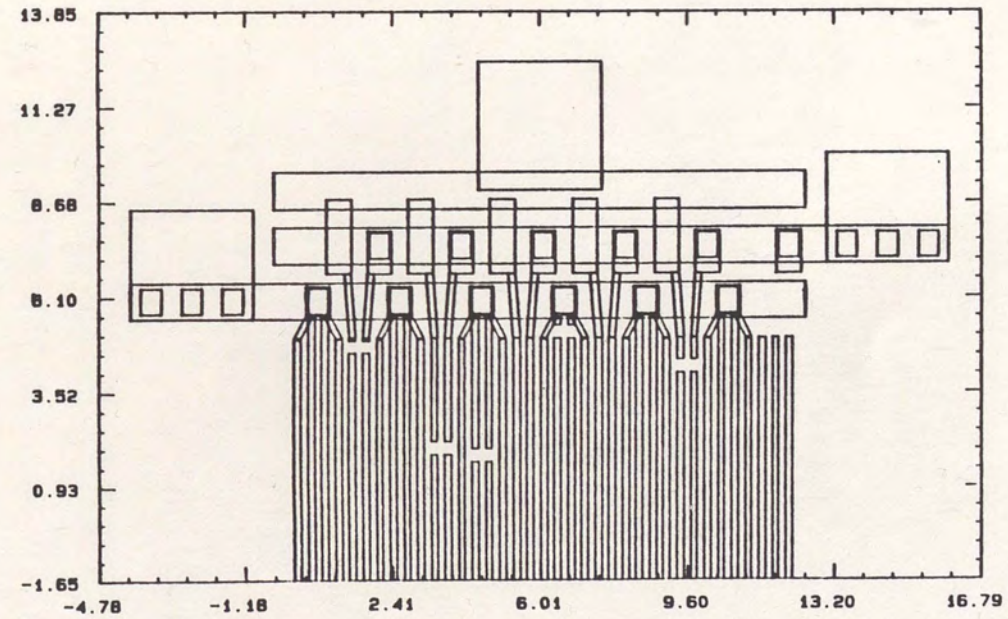

Figure 7.5(b). Close-up of Sample Apodized UDT, All Mask Levels Shown.

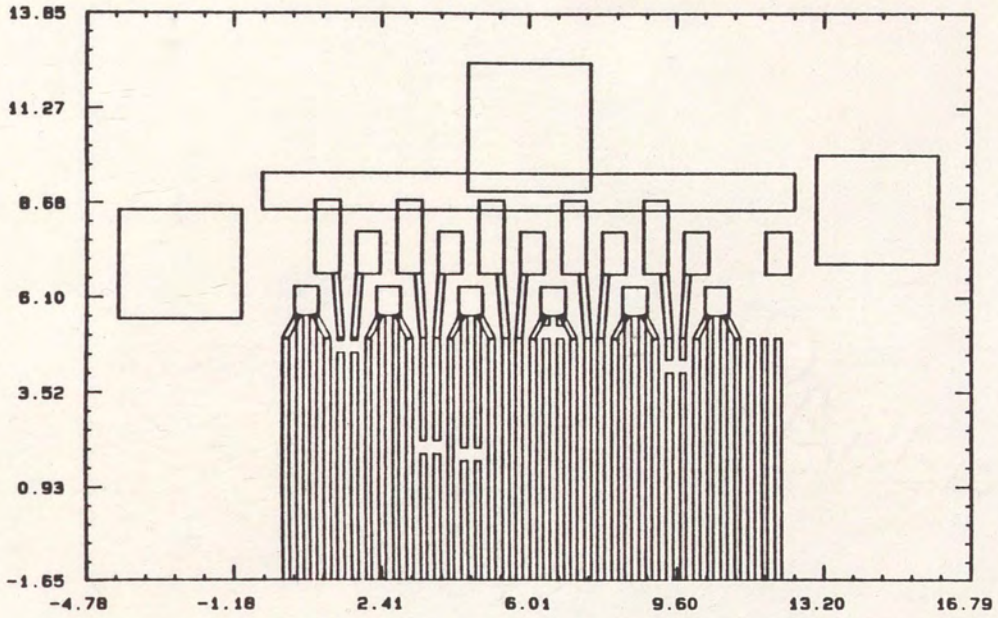

Figure 7.6(a). First Mask Level of the Sample UDT.

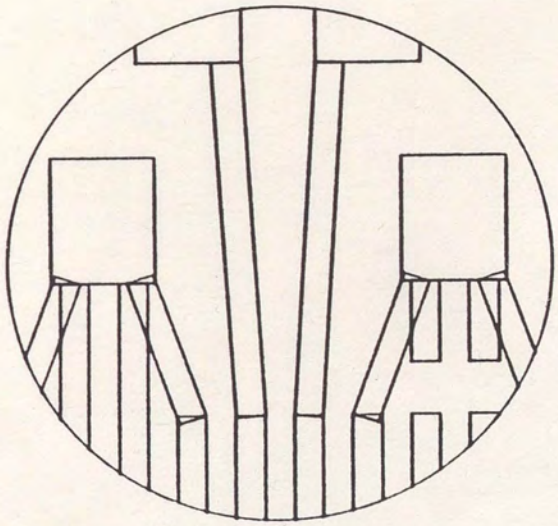

Figure 7.6(b). Spanning of Electrodes.

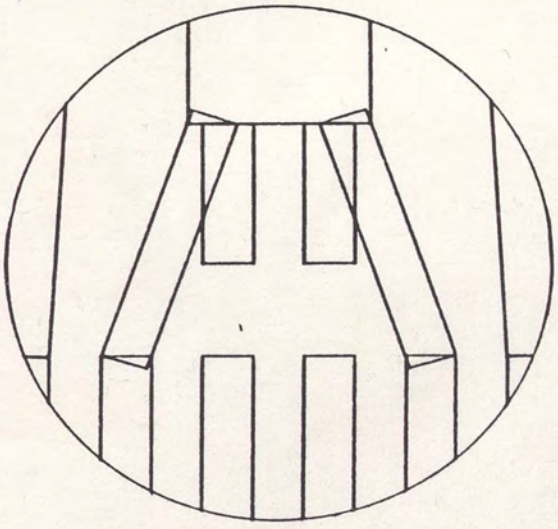

Figure 7.6(c). Overlap of Electrodes.

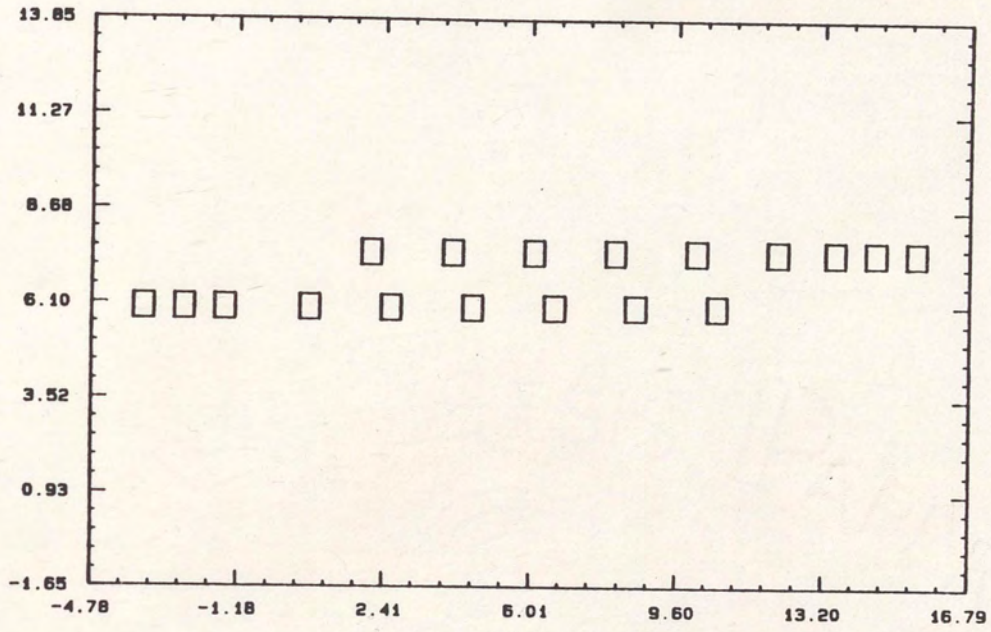

Figure 7.7. Second Mask Level of Sample UDT.

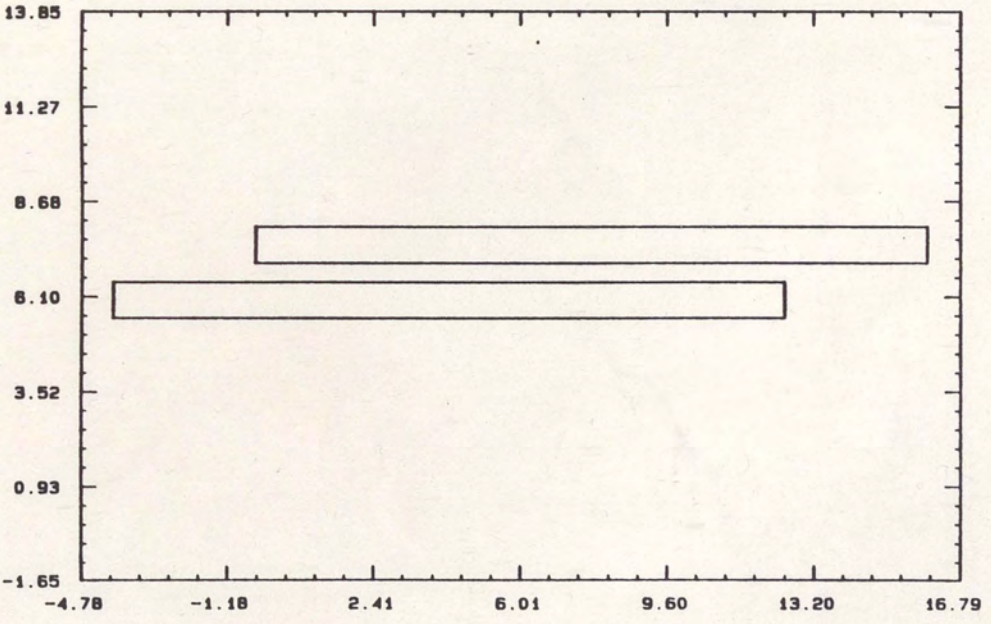

Figure 7.8. Third Mask Level of Sample UDT.

Note that three via holes are used to make contact between the bond pads and the crossovers. This is done to help minimize resistive losses to the crossover connections. The crossovers only make contact along the edge of the via holes. Therefore, the resistive losses of the crossovers may be reduced if the total perimeter of the via holes is increased. If the width of the via holes were made slimmer or the bond pad longer, then more via holes could be added to the bond pads and the total perimeter of the connection to the bond pad would be increased, thereby reducing resistive losses.

Figure 7.8 illustrates a phase change in a structure. The phase change is implemented spatially by placing a half wavelength gap in the structure. This gap may be seen in the center of Figure 7.9.

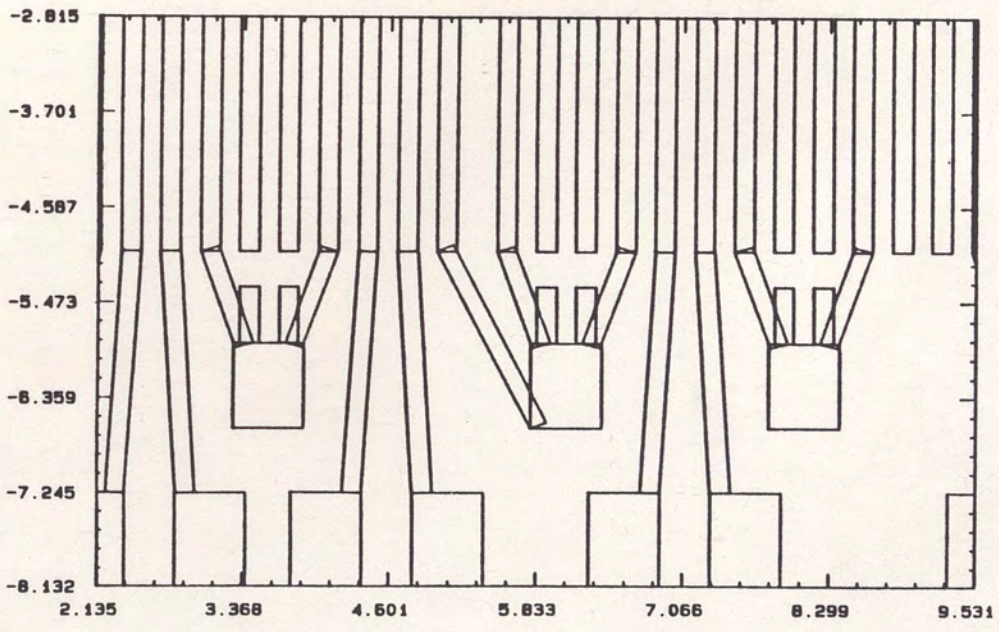

Figure 7.9. Structure with a Phase Change.

CHAPTER VIII

CONCLUSIONS

A novel apodization technique for the apodization of three phase unidirectional transducers was presented. This structure was compared to a previously reported [7] apodization technique for UDTs and was shown to have several superior characteristics.

For the purpose of comparing the performance of the two structures, SAWCAD2 was updated to perform channel analysis of UDTs. Corrections to the element and array factors were also added.

The new structure was shown to have a capacitively balanced equivalent network, where that of the previously reported structure does not. The apodization loss of the balanced structure was also shown to be significantly less than that of the unbalanced structure. A significant advantage of the balanced structure over an unbalanced structure is the reduction of passband ripple and distortion in the complete transducer response due to the lesser degree of ripple present in that structure's conductance.

Finally, a FORTRAN-77 program was written and described for implementation of the three mask levels required to fabricate the balanced three phase unidirectional transducers, given a general impulse response.

Further work on the apodization of three phase unidirectional transducers should include the fabrication of devices for the purpose of experimentally verifying the results of the analysis presented. The experimental work should concentrate on the areas of conductance and narrowband frequency response measurements since these were the areas which differed significantly between the two apodization patterns.

APPENDIX

SUMMARY OF A UDT FABRICATION PROCEDURE

This summary presents a short and simple method of fabricating a three phase UDT for conceptual purposes only. It is not meant to be detailed and should not be used as a guide for the fabrication of such devices.

The fabrication of a three phase transducer requires crossovers, and as a result, three mask levels are necessary for the fabrication of such a device. The first mask is used in the generation of the metalized electrode patterns as well as the crossover pads and bond pads. The second is used in opening the via holes in the dielectric so that the crossover metal bridges may make contact with the first level metal crossover pads. The third and last mask is used to generate the crossovers.

The following list is a short summary of a procedure for the fabrication of a three phase UDT:

1. Clean the piezo electric substrate.
2. Deposit a layer of metalization to the substrate.
3. Apply photoresist to the metalized substrate.
4. Expose the photoresist using mask #1.
5. Develop the photoresist.
6. Etch the metal, leaving behind the electrodes, crossover pads and bond pads.
7. Strip off the remaining photoresist.

8. Apply a layer of dielectric over the metalization pattern.

9. Apply photoresist to the dielectric.

10. Expose the photoresist using mask #2.

11. Develop the photoresist.

12. Etch the dielectric, opening the via holes for the crossovers.

13. Strip off the remaining photoresist.

14. Deposit a thick layer of metalization. These metalizations shall be used for the crossovers and it is necessary that this layer of metal be thick enough to structurally support the crossovers.

15. Apply photoresist to the metal.

16. Expose the photoresist using mask #3.

17. Develop the photoresist.

18. Etch the metal, leaving behind the crossovers.

19. Strip off the remaining photoresist.

20. Strip off the remaining dielectric leaving behind the air gap crossovers. These crossovers resemble small bridges interconnecting the bond pads with the crossover pads.

21. Clean the device.

22. Mount and bond the device.

23. Externally connect the necessary phasing and matching networks to the device.

24. The device is now ready for testing.

REFERENCES

1. Hartman, Clinton S.; Wright, P.V.; Kansy, R.J.; and Garber, E.M. "Wideband Unidirectional Interdigital Surface Wave Transducers." IEEE Transactions on Sonics and Ultrasonics 19 (July 1972): 378-381.

2. Collins, J.H.; Gerard, H.M.; Reeder, T.M.; and Shaw, H.M. "Unidirectional Surface Wave Transducer." Proceedings of the IEEE (1969): 833-835.

3. Qui, P.; Shui, Y.; Chang, D.; Wenhua, J.; and Wenqui, W. "Wideband Low Loss Surface Acoustic Wave Filters." IEEE Ultrasonics Symposium Proceedings (1981): 164-169.

4. Malocha, D.C. "Quadrature Three Phase Unidirectional Transducer." IEEE Transactions on Sonics and Ultrasonics 26 (July 1979): 313-315.

5. Wright, P.V. "The Natural Single Phase Unidirectional Transducer: A New Low Loss Saw Transducer." IEEE Ultrasonics Symposium Proceedings (1985): preprint.

6. Hartman, Clinton S. "Weighting Interdigital Surface Wave Transducers by Selective Withdrawal of Electrodes." IEEE Ultrasonics Symposium Proceedings (1973): 423-426.

7. Peach, R.C., and Dix, C. "A Low Loss Medium Bandwidth Filter on Lithium Niobate." IEEE Ultrasonics Symposium Proceedings (1978): 509-512.

8. Waldron, R.A. "Power Transfer Factors for Nonuniformly Irradiated Interdigital Piezoelectric Transducers." IEEE Transactions on Sonics and Ultrasonics 19 (October 1972): 448-453.

9. Malocha, D.C., and Richie, S.M. "Computer Aided Design and Analysis of Surface Acoustic Wave Three Phase Unidirectional Transducers." Unpublished Technical Report, University of Central Florida, June 1984.

10. Datta, Supriyo, and Hunsinger, Bill J. "Element Factor for Periodic Transducers." IEEE Transactions on Sonics and Ultrasonics 27 (January 1980): 42-44.

11. Ristic, Velimir M. Principles of Acoustic Devices. New York: John Wiley and Sons, Inc., 1983.

12. Rosenfeld, R.C.; Brown, R.B.; and Hartman, C.S. "Unidirectional Acoustic Surface Wave Filters with 2 dB Insertion Loss." IEEE Ultrasonics Symposium Proceedings (1974): 425-428.

13. Richie, Samuel M. "Three Phase Unidirectional Surface Acoustic Wave Transducer Model and Computer Aided Design Implementation." Master's Thesis, University of Central Florida, Orlando, 1983.

14. Richie, Samuel M. Private communication. College of Engineering, University of Central Florida, Orlando, November 1985.

15. Malocha, Donald C. Private communication. College of Engineering, University of Central Florida, Orlando, August 1985.

16. Bishop, Carlton D. "Non-iterative Design of Finite Impulse Response Filters." Master's Thesis, University of Central Florida, Orlando, 1985.

17. Hartman, Clinton S.; Bell, Delamar T.; and Rosenfeld, Ronald C. "Impulse Model Design of Acoustic Surface-Wave Filters." IEEE Transactions on Microwave Theory and Techniques 21 (April 1973): 162-175.